Chinese Journal of Chemical Engineering 76 (2024) 83–94

Contents lists available at ScienceDirect

Chinese Journal of Chemical Engineering

journal homepage: www.elsevier.com/locate/CJChE

Full Length Article

Solid–liquid phase equilibria in the aqueous system containing the chlorides of potassium, ammonium, and calcium at 298.2, 323.2, and 348.2 K

Fuyu Zhuge [1], Nan Zhang [1], Haiying Tang [1,2], Qi Li [1], Niancu Chen [1], Xudong Yu [1,*]

[1] College of Materials and Chemistry & Chemical Engineering, Chengdu University of Technology, Chengdu 610059, China
[2] Qinghai Salt Lake Industry Co., Ltd., Golmud 816000, China

A R T I C L E I N F O

Article history:
Received 1 July 2024
Received in revised form
6 August 2024
Accepted 12 August 2024
Available online 4 October 2024

Keywords:
Phase equilibria
Solubility
Hydrate
Deep brine
Double salt
Solid solution

A B S T R A C T

In order to obtain the crystalline forms of the salts of the potassium, ammonium, calcium coexisting chloride system, the phase equilibria relationship of quaternary system K^+, NH_4^+, Ca^{2+}//Cl^--H_2O at 298.2, 323.2, and 348.2 K was studied by isothermal dissolution equilibrium method. The solubility and density of equilibrium liquid phases of the system were experimentally determined; X-ray powder diffractometer was used to determine the compositions of the equilibrium solid phase at the quaternary invariant point. It is found that the quaternary system is a complex system at these three temperatures. The phase diagram at 298.2 K consists of three invariant points, seven univariate curves and five crystalline phase regions, forming the solid solutions $(NH_4Cl)_x(KCl)_{1-x}$ and $(KCl)_x(NH_4Cl)_{1-x}$; while at 323.2 and 348.2 K the phase diagram consists of five invariant points, eleven univariate curves and seven crystalline phase regions, the double salts ($KCl\cdot CaCl_2$) and ($2NH_4Cl\cdot CaCl_2\cdot 3H_2O$), solid solutions $(KCl)_x(NH_4Cl)_{1-x}$ and $(NH_4Cl)_x(KCl)_{1-x}$ were formed. Among them, the crystalline phase region of solid solution $(KCl)_x(NH_4Cl)_{1-x}$ is the largest at three temperatures, indicating that it is the easiest to crystallize in this system. Comparing the phase diagrams of the quaternary system at 298.2, 323.2, and 348.2 K, it can be seen that the crystalline form of $CaCl_2$ changes with the increase of temperature: $CaCl_2\cdot 6H_2O$ at 298.2 K, $CaCl_2\cdot 2H_2O$ at 323.2 and 348.2 K. From 323.2 to 348.2 K, the crystalline phase regions of ($KCl\cdot CaCl_2$) and ($2NH_4Cl\cdot CaCl_2\cdot 3H_2O$) increased gradually.

1. Introduction

China is a large agricultural country, and also a big country of potassium salt consumption and import. The rational exploitation and utilization of potassium salt is directly related to national food security [1,2]. The global potash (potassium chloride equivalent) reserves are 14.9 billion tons, and the resources are 69 billion tons, mainly distributed in Russia, Canada, Belarus, and Turkmenistan. China's potash reserves are 170 million tons, accounting for only 5.15% of the world's total potash reserves [3]. The occurrence form of potassium resources in China has its particularity, 98% of the proven potassium resources are abundant in liquid brine potassium deposits, which mainly distributed in salt lake brines in Qinghai, Xinjiang and Xizang [4,5], as well as deep brine represented by Sichuan Basin, Jianghan Basin and Qaidam Basin [6–8]. Among them, the concentration of K^+, $Ca^{2+}$and NH_4^+ in the Xuanhan deep brine in Northeast Sichuan is 25.955, 10.877, and 0.816 $g\cdot L^{-1}$ [6]. Nanyishan deep brine in the Qaidam Basin is a calcium chloride type with high salinity (118.2–287.9 $g\cdot L^{-1}$), high calcium (14.73–16.09 $g\cdot L^{-1}$), and the content of potassium is 5.21–7.66 $g\cdot L^{-1}$, ammonium is 0.143 $g\cdot L^{-1}$ [9], which has high development and utilization value. In addition, due to the particularity of its occurrence state, deep brine has the characteristics of deep burial and high brine temperature. For example, the burial depth of brine in northeastern Sichuan is 1000–3260 m, the occurrence temperature of brine is mostly concentrated in 296.2–348.2 K. At the same time, the deep brine also contains ammonium and calcium, which is significantly different from the salt lake brine system and seawater system, it may form double salts or solid solutions with coexisting potassium, which makes the ion interaction relationship complex and increases the difficulty of salt separation. Therefore, to obtain the salt interaction relationship

* Corresponding author.
E-mail address: xwdlyxd@126.com (X. Yu).

https://doi.org/10.1016/j.cjche.2024.08.010
1004-9541/

of the chlorides type solution containing potassium, ammonium and calcium at multi-temperature, the phase equilibria of system K^+, NH_4^+, Ca^{2+}//Cl^--H_2O is necessary.

By analyzing the existing literature related to the system, it can be seen that: for the potassium-ammonium system, system K^+, NH_4^+//Cl^--H_2O [10–12], Li^+, K^+, NH_4^+//Cl^--H_2O [13], K^+, NH_4^+, Ca^{2+}//Cl^--H_2O [14], K^+, NH_4^+, Mg^{2+}//Cl^--H_2O [15–17] are all complex system with solid solutions $(KCl)_x(NH_4Cl)_{1-x}$ and $(NH_4Cl)_x(KCl)_{1-x}$ formed. For system K^+, Ca^{2+}//Cl^--H_2O, our group has carried out phase equilibria at 278.2–348.2 K [18,19], it is a simple system at 278.2–308.2 K; while at 323.2 and 348.2 K, they are complex system with double salt ($KCl\cdot CaCl_2$) formed. For the ammonium-calcium system, the system NH_4^+, Ca^{2+}//Cl^--H_2O [20–22] has no double salt at 298.2 K, while it is a complex system with $2NH_4Cl\cdot CaCl_2\cdot 3H_2O$ formed at 308.2, 323.2, and 348.2 K. As for quaternary system NH_4^+, Ca^{2+}, Al^{3+}//Cl^--H_2O at 298.2 K [23], NH_4^+, Ca^{2+}, Sr^{2+}//Cl^--H_2O at 298.2 K [24] without double salt found. The double salt $2NH_4Cl\cdot CaCl_2\cdot 3H_2O$ formed in the system NH_4^+, Mg^{2+}, Ca^{2+}//Cl^--H_2O at 323.2 K [25]. Analysis of the above literature found that both temperature and coexisting ions have an effect on the crystal form of salt in the potassium ammonium calcium coexisting chloride system. Therefore, combined with the temperature characteristics of deep brine, the phase equilibria of the K^+, NH_4^+, Ca^{2+}//Cl^--H_2O at 298.2, 323.2, and 348.2 K were studied by isothermal dissolution equilibrium method, and the multi-temperature comparison was carried out.

2. Experimental

2.1. Reagents

The ultrapure water with $\kappa \le 5.5 \times 10^{-6}\ S\cdot m^{-1}$ was obtained by ultra-pure water equipment. The single element standard solutions of potassium, ammonium and calcium were all from the National Nonferrous Metals and Electronic Materials Analysis and Testing Center. The main experimental reagent is listed in Table 1.

2.2. Instruments

The main equipment used in phase equilibrium experimental research, phase identification and composition analysis are listed in Table 2.

2.3. Experimental method

The phase equilibrium of quaternary system K^+, NH_4^+, Ca^{2+}//Cl^--H_2O was studied by the isothermal dissolution equilibrium method. Based on the invariant point data of each ternary subsystems at 298.2, 323.2, and 348.2 K, a series of ternary saturated solutions with the same composition were prepared. Add a third new salt to the above solutions according to the mass gradient to form a series of samples with different compositions. The sample is placed in a cyclotron oscillator to oscillate to speed up the equilibrium. The oscillator is placed in the thermostat to control the system temperature, and the supernatant was analyzed regularly. When the composition of the sample was unchanged, the system was considered to be equilibrated (the equilibrium time was about 30 d). After the system reached equilibrium, stopped the oscillation, and the sample was placed in a thermostat for 48 h, followed by solid-liquid separation. The composition and density of the equilibrium liquid phase were measured. The equilibrium solid phase composition was analyzed by X-ray powder diffraction. The following are analytical methods for each ion: K^+: Atomic absorption spectrophotometry (AAS), standard uncertainty ± 0.30% [26]; NH_4^+: Ion chromatography, standard uncertainty±0.31% [27]; Ca^{2+}: Atomic absorption spectrophotometry (AAS), standard uncertainty±0.30% [28], EDTA standard solution titration, standard uncertainty±0.46% [29]; Cl^-: $AgNO_3$ titration method with K_2CrO_4 as indicator, standard uncertainty±0.30% [29]. Three parallel measurements were performed, and the average value was taken as the final result.

3. Results and Discussion

The solubility of the K^+, NH_4^+, Ca^{2+}//Cl^--H_2O was expressed by mass fraction w(B) and Jänecke index J(B) (g/100 g dry salt) (B=KCl, NH_4Cl, $CaCl_2$, H_2O). The calculation formula of J(B) is shown in Eqs. (1)–(5).

$$w_s = w_{KCl} + w_{NH_4Cl} + w_{CaCl_2} \tag{1}$$

$$J(KCl) = w_{KCl}/w_s \times 100 \tag{2}$$

$$J(NH_4Cl) = w_{NH_4Cl} \,/\, w_s \times 100 \tag{3}$$

Table 1
Reagents of the experiment

Reagent	CAS no.	Initial purity/% (mass)	Purified method	Final purity/% (mass)	Manufacturer
KCl	7447-40-7	99.5	recrystallization	99.8	Tianjin Kermel Chemicals Reagents Co., Ltd., China
NH_4Cl	12125-02-9	99.0	recrystallization	99.8	Chengdu Chron Chemicals Co., Ltd., China
$CaCl_2$	10043-52-4	99.9	–	–	Shanghai Boer Chemical Reagents Co., Ltd., China

Table 2
Instruments of the experiment

Instruments	Instrument type	Manufacturer
Analytical balance	BSA124S	Sartorius Scientific Instruments (Beijing) Co., Ltd.
Thermostat	SHH-250	Chongqing Inborn Experiment Instrument, China
Thermostat oscillator	HY-5B	Changzhou Hongke Instrument Factory
Atomic absorption spectrophotometry	iCE 3300	Thermo Fisher Technology Co., Ltd.
X-ray diffractometer	ULTIMAIV X	Neo-Japanese Science Corporation
Ion chromatography	CIC-100	Qingdao Shenghan Chromatographic Technology Co., Ltd.
Ultra-pure water system	UPT-II-20T	Sichuan Youpu Ultra-pure Technology Co., Ltd.

Table 3
The experimental date (solubilities, density) of solid−liquid equilibria of the quaternary system K^+, NH_4^+, Ca^{2+}//Cl^--H_2O at 298.2 K

No.	Density, ρ/g·cm^{-3}	Equilibrium solutions composition, w(B)/%				Jänecke index of dry salt, J(B) (g/100 g S)/g·g^{-1}				Equilibrium solid phase (Sal: NH_4Cl, Ant: $CaCl_2 \cdot 6H_2O$)
						$J(KCl) + J(NH_4Cl) + J(CaCl_2) = 100$				
		$w(KCl)$	$w(NH_4Cl)$	$w(CaCl_2)$	$w(H_2O)$	$J(KCl)$	$J(NH_4Cl)$	$J(CaCl_2)$	$J(H_2O)$	
1, A	1.1015	6.17	24.82	0.00	69.01	19.91	80.09	0.00	222.68	Sal+$(NH_4Cl)_x(KCl)_{1-x}$
2	1.1141	6.01	24.24	0.70	69.05	19.44	78.32	2.25	223.11	Sal+$(NH_4Cl)_x(KCl)_{1-x}$
3	1.1277	5.90	21.66	3.69	68.74	18.89	69.31	11.80	219.93	Sal+$(NH_4Cl)_x(KCl)_{1-x}$
4	1.1442	4.90	19.80	6.72	68.58	15.59	63.03	21.38	218.27	Sal+$(NH_4Cl)_x(KCl)_{1-x}$
5	1.1591	5.15	17.76	9.29	67.80	15.98	55.17	28.85	210.55	Sal+$(NH_4Cl)_x(KCl)_{1-x}$
6	1.1839	4.82	14.85	12.98	67.35	14.77	45.49	39.75	206.25	Sal+$(NH_4Cl)_x(KCl)_{1-x}$
7	1.2013	4.57	14.19	14.64	66.60	13.69	42.47	43.83	199.37	Sal+$(NH_4Cl)_x(KCl)_{1-x}$
8	1.2184	4.44	12.02	17.43	66.11	13.09	35.48	51.44	195.09	Sal+$(NH_4Cl)_x(KCl)_{1-x}$
9	1.2463	4.27	11.83	17.93	65.97	12.54	34.77	52.70	193.82	Sal+$(NH_4Cl)_x(KCl)_{1-x}$
10	1.2890	4.17	9.09	22.67	64.07	11.61	25.30	63.09	178.30	Sal+$(NH_4Cl)_x(KCl)_{1-x}$
11, X_1	1.2917	4.16	8.47	23.90	63.47	11.38	23.17	65.44	173.76	Sal+$(NH_4Cl)_x(KCl)_{1-x}$+$(KCl)_x(NH_4Cl)_{1-x}$
12, B	1.1294	11.42	21.84	0.00	66.74	34.34	65.66	0.00	200.66	$(NH_4Cl)_x(KCl)_{1-x}$+$(KCl)_x(NH_4Cl)_{1-x}$
13	1.1378	10.88	21.26	0.88	66.98	32.96	64.38	2.67	202.84	$(NH_4Cl)_x(KCl)_{1-x}$+$(KCl)_x(NH_4Cl)_{1-x}$
14	1.1439	10.56	20.46	2.05	66.94	31.93	61.87	6.20	202.45	$(NH_4Cl)_x(KCl)_{1-x}$+$(KCl)_x(NH_4Cl)_{1-x}$
15	1.1478	10.46	19.18	3.46	66.90	31.60	57.96	10.45	202.10	$(NH_4Cl)_x(KCl)_{1-x}$+$(KCl)_x(NH_4Cl)_{1-x}$
16	1.1605	9.91	17.84	5.36	66.88	29.93	53.88	16.20	201.95	$(NH_4Cl)_x(KCl)_{1-x}$+$(KCl)_x(NH_4Cl)_{1-x}$
17	1.1665	9.42	17.28	6.62	66.68	28.27	51.86	19.86	200.09	$(NH_4Cl)_x(KCl)_{1-x}$+$(KCl)_x(NH_4Cl)_{1-x}$
18	1.1821	8.09	14.99	10.36	66.56	24.19	44.82	30.99	199.06	$(NH_4Cl)_x(KCl)_{1-x}$+$(KCl)_x(NH_4Cl)_{1-x}$
19	1.1956	7.34	13.66	12.74	66.26	21.76	40.48	37.75	196.41	$(NH_4Cl)_x(KCl)_{1-x}$+$(KCl)_x(NH_4Cl)_{1-x}$
20	1.2153	6.61	13.03	14.40	65.96	19.41	38.27	42.31	193.78	$(NH_4Cl)_x(KCl)_{1-x}$+$(KCl)_x(NH_4Cl)_{1-x}$
21	1.2350	5.72	11.16	18.11	65.00	16.36	31.90	51.75	185.72	$(NH_4Cl)_x(KCl)_{1-x}$+$(KCl)_x(NH_4Cl)_{1-x}$
22	1.2587	5.23	10.65	19.13	64.99	14.95	30.41	54.64	185.61	$(NH_4Cl)_x(KCl)_{1-x}$+$(KCl)_x(NH_4Cl)_{1-x}$
23	1.2707	4.66	9.59	21.53	64.22	13.03	26.81	60.16	179.45	$(NH_4Cl)_x(KCl)_{1-x}$+$(KCl)_x(NH_4Cl)_{1-x}$
24	1.3011	3.88	8.00	24.97	63.15	10.52	21.72	67.76	171.40	Sal+$(KCl)_x(NH_4Cl)_{1-x}$
25	1.3217	3.53	7.44	27.04	61.98	9.30	19.58	71.12	163.05	Sal+$(KCl)_x(NH_4Cl)_{1-x}$
26	1.3371	3.22	6.81	29.36	60.61	8.18	17.30	74.53	153.86	Sal+$(KCl)_x(NH_4Cl)_{1-x}$
27	1.3540	3.02	6.43	30.53	60.03	7.55	16.08	76.37	150.17	Sal+$(KCl)_x(NH_4Cl)_{1-x}$
28	1.3508	2.77	5.86	31.33	60.04	6.93	14.67	78.40	150.26	Sal+$(KCl)_x(NH_4Cl)_{1-x}$
29	1.3763	2.55	5.30	34.69	57.46	5.99	12.46	81.55	135.07	Sal+$(KCl)_x(NH_4Cl)_{1-x}$
30, X_2	1.4608	2.66	5.38	41.82	50.15	5.33	10.79	83.89	100.59	Sal+$(KCl)_x(NH_4Cl)_{1-x}$ + Ant
31, C	1.1697	23.74	3.40	0.00	72.86	87.47	12.53	0.00	268.46	$(KCl)_x(NH_4Cl)_{1-x}$ + KCl
32	1.1696	22.46	3.68	0.69	73.17	83.71	13.72	2.57	272.70	$(KCl)_x(NH_4Cl)_{1-x}$ + KCl
33	1.1753	20.94	3.63	2.19	73.24	78.25	13.57	8.18	273.69	$(KCl)_x(NH_4Cl)_{1-x}$ + KCl
34	1.1782	19.51	3.51	3.75	73.24	72.89	13.11	14.00	273.65	$(KCl)_x(NH_4Cl)_{1-x}$ + KCl
35	1.1851	18.01	3.48	5.60	72.91	66.50	12.84	20.67	269.19	$(KCl)_x(NH_4Cl)_{1-x}$ + KCl
36	1.1888	17.74	3.08	6.68	72.51	64.52	11.19	24.29	263.78	$(KCl)_x(NH_4Cl)_{1-x}$ + KCl
37	1.1979	14.96	3.01	10.05	71.98	53.40	10.74	35.86	256.83	$(KCl)_x(NH_4Cl)_{1-x}$ + KCl
38	1.2060	14.85	2.74	11.29	71.11	51.42	9.49	39.10	246.15	$(KCl)_x(NH_4Cl)_{1-x}$ + KCl
39	1.2236	12.18	2.58	14.97	70.27	40.97	8.67	50.36	236.40	$(KCl)_x(NH_4Cl)_{1-x}$ + KCl
40	1.2343	9.17	2.69	18.39	69.75	30.31	8.90	60.79	230.56	$(KCl)_x(NH_4Cl)_{1-x}$ + KCl
41	1.2589	8.07	2.52	19.46	69.95	26.85	8.40	64.75	232.80	$(KCl)_x(NH_4Cl)_{1-x}$ + KCl
42	1.2760	6.63	2.34	22.38	68.66	21.14	7.45	71.40	219.06	$(KCl)_x(NH_4Cl)_{1-x}$ + KCl
43	1.2946	5.47	2.26	25.29	66.97	16.56	6.86	76.59	202.78	$(KCl)_x(NH_4Cl)_{1-x}$ + KCl
44	1.3212	5.09	2.14	26.96	65.81	14.90	6.25	78.85	192.44	$(KCl)_x(NH_4Cl)_{1-x}$ + KCl
45	1.3319	4.80	2.11	27.91	65.18	13.79	6.06	80.15	187.19	$(KCl)_x(NH_4Cl)_{1-x}$ + KCl
46	1.3306	4.46	2.15	28.83	64.56	12.57	6.07	81.36	182.17	$(KCl)_x(NH_4Cl)_{1-x}$ + KCl
47	1.3439	3.98	2.07	30.44	63.52	10.90	5.66	83.44	174.14	$(KCl)_x(NH_4Cl)_{1-x}$ + KCl
48	1.3494	3.48	2.04	31.25	63.22	9.46	5.56	84.98	171.90	$(KCl)_x(NH_4Cl)_{1-x}$ + KCl
49	1.3630	3.20	1.91	33.33	61.57	8.31	4.97	86.72	160.19	$(KCl)_x(NH_4Cl)_{1-x}$ + KCl
50	1.3806	2.86	1.88	36.49	58.76	6.94	4.57	88.49	142.48	$(KCl)_x(NH_4Cl)_{1-x}$ + KCl
51, X_3	1.4784	3.44	2.47	44.16	49.93	6.87	4.94	88.19	99.71	$(KCl)_x(NH_4Cl)_{1-x}$ + KCl + Ant
52, D	1.5404	2.86	0.00	45.68	51.46	5.89	0.00	94.11	106.02	KCl + Ant
53	1.4812	3.43	0.80	44.68	51.09	7.00	1.64	91.35	104.44	KCl + Ant
54	1.4747	3.60	1.37	44.77	50.26	7.24	2.76	90.00	101.03	KCl + Ant
55	1.4802	3.51	1.90	44.64	49.95	7.02	3.80	89.18	99.79	KCl + Ant
56	1.4556	2.87	3.04	41.62	52.46	6.05	6.40	87.55	110.35	$(KCl)_x(NH_4Cl)_{1-x}$ + Ant
57	1.4479	2.58	4.04	42.26	51.13	5.27	8.26	86.47	104.62	$(KCl)_x(NH_4Cl)_{1-x}$ + Ant
58	1.4561	2.49	4.65	42.10	50.77	5.05	9.44	85.51	103.12	$(KCl)_x(NH_4Cl)_{1-x}$ + Ant
59	1.4682	2.20	5.57	43.89	48.33	4.27	10.78	84.95	93.54	Sal + Ant
60	1.4630	1.03	5.66	44.17	49.14	2.02	11.13	86.86	96.62	Sal + Ant
61	1.4544	0.47	5.69	44.62	49.22	0.92	11.21	87.87	96.92	Sal + Ant
62, E	1.3815	0.00	5.39	41.64	52.97	0.00	11.46	88.54	112.63	Sal + Ant

Note: Standard uncertainties u are $u(T) = 0.20$ K, $u(\rho) = 0.0002$ g·cm^{-3}; the relative standard uncertainties u_r are $u_r(w(KCl)) = 0.0030$, $u_r(w(NH_4Cl)) = 0.0031$, and $u_r(w(CaCl_2)) = 0.0046$.

$$J(CaCl_2) = w_{CaCl_2} / w_s \times 100 \tag{4}$$

$$J(H_2O) = w_{H_2O} / w_s \times 100 \tag{5}$$

3.1. The phase diagram of quaternary system K^+, NH_4^+, Ca^{2+}//Cl^--H_2O at 298.2 K

The experimental data of the quaternary system was listed in Table 3. The equilibrium phase diagram of the system was drawn according to the data in Fig. 1. The phase diagram consists of three invariant points, seven univariate curves and five crystallization phase regions.

The XRD identification spectrum of the invariant point X_1 can be seen in Fig. 2. The X-ray diffraction peaks are compared with the standard cards of KCl and NH_4Cl, the diffraction peaks of KCl at 2θ 40°–50°, 50°–60°, and 60°–70° are shifted to the left, indicating that there is a solid solution $(KCl)_x(NH_4Cl)_{1-x}$ formed by point substitution of NH_4^+ into KCl crystal in the system. The diffraction peaks of NH_4Cl at 2θ 20°–30° and 30°–40° shifted to the right. Therefore, it can be inferred that there is a solid solution $(NH_4Cl)_x(KCl)_{1-x}$ in the equilibrium solid phase from K^+ into the NH_4Cl crystal, and the composition of the invariant point X_1 is $(NH_4Cl)_x(KCl)_{1-x}$, $(KCl)_x(NH_4Cl)_{1-x}$, and NH_4Cl, the corresponding liquid phase composition is $w(KCl) = 4.16\%$, $w(NH_4Cl) = 8.47\%$, $w(CaCl_2) = 23.90\%$, $w(H_2O) = 63.47\%$.

The XRD spectrum of X_2 is shown in Fig. 3. It is found that the diffraction peaks of KCl at 2θ 40°–50° and 50°–60° are shifted to the left, indicating the presence of $(KCl)_x(NH_4Cl)_{1-x}$ in the solid phase. At the same time, the diffraction peaks are in good agreement with $CaCl_2 \cdot 6H_2O$ and NH_4Cl. Therefore, it is inferred that the equilibrium solid phase of the invariant point X_2 is NH_4Cl, $(KCl)_x(NH_4Cl)_{1-x}$, and $CaCl_2 \cdot 6H_2O$, the equilibrium liquid phase composition is $w(KCl) = 2.66\%$, $w(NH_4Cl) = 5.38\%$, $w(CaCl_2) = 41.82\%$, $w(H_2O) = 50.15\%$.

The XRD pattern of X_3 is shown in Fig. 4. The equilibrium solid phase composition of the invariant point X_3 is $(KCl)_x(NH_4Cl)_{1-x}$, $CaCl_2 \cdot 6H_2O$, and KCl, the equilibrium liquid phase composition is $w(KCl) = 3.44\%$, $w(NH_4Cl) = 2.47\%$, $w(CaCl_2) = 44.16\%$, $w(H_2O) = 49.93\%$.

The seven univariate curves and their corresponding solid phases are as follows, AX_1: NH_4Cl+$(NH_4Cl)_x(KCl)_{1-x}$; BX_1: $(NH_4Cl)_x$

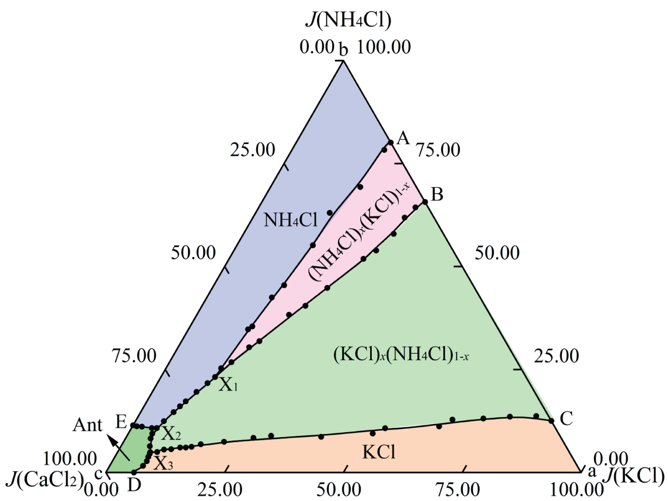

Fig. 1. Phase diagram of quaternary system K^+, NH_4^+, Ca^{2+}//Cl^--H_2O 298.2 K (Ant: $CaCl_2 \cdot 6H_2O$).

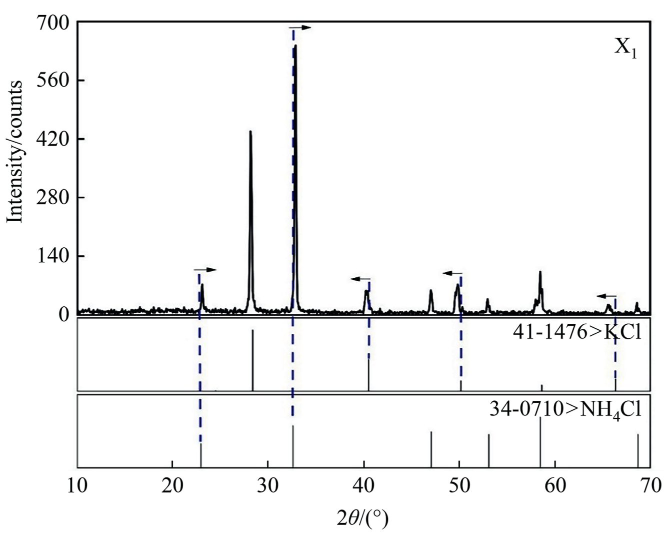

Fig. 2. The XRD pattern of the invariant point X_1.

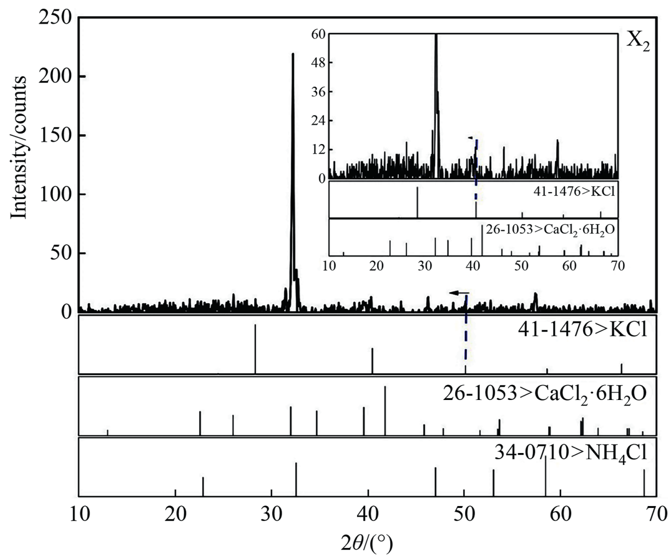

Fig. 3. The XRD pattern of the invariant point X_2.

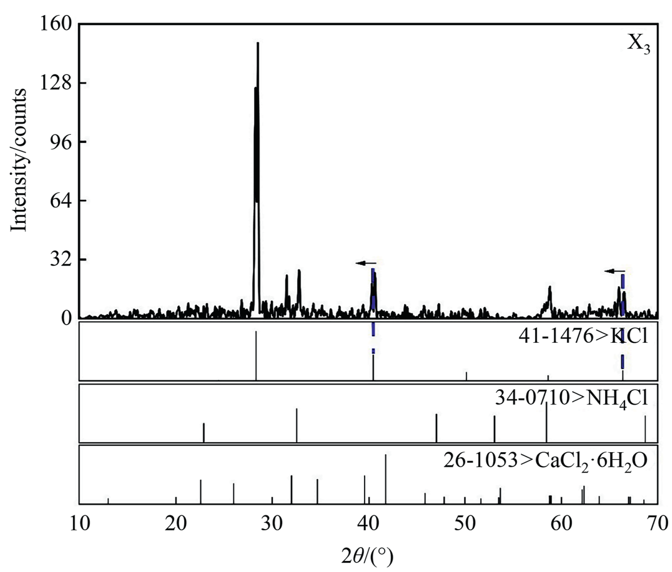

Fig. 4. The XRD pattern of the invariant point X_3.

$(KCl)_{1-x}$+$(KCl)_x(NH_4Cl)_{1-x}$; X_1X_2: NH_4Cl+$(KCl)_x(NH_4Cl)_{1-x}$; EX_2: NH_4Cl + $CaCl_2\cdot 6H_2O$; X_2X_3: $CaCl_2\cdot 6H_2O$+$(KCl)_x(NH_4Cl)_{1-x}$; CX_3: $(KCl)_x(NH_4Cl)_{1-x}$ + KCl; DX_3: KCl + $CaCl_2\cdot 6H_2O$.

There are five crystallization phase regions in the phase diagram. Two solid solution crystalline regions: $[(NH_4Cl)_x(KCl)_{1-x}]$ (AX_1BA), $[(KCl)_x(NH_4Cl)_{1-x}]$($BX_1X_2X_3CB$); Three single salt crystalline regions: NH_4Cl(bEX_2X_1Ab), KCl(aDX_3Ca) and $CaCl_2\cdot 6H_2O$ (cDX_3X_2Ec). The area of the crystallization regions decreases in the order of $(KCl)_x(NH_4Cl)_{1-x}$, NH_4Cl, KCl, $(NH_4Cl)_x(KCl)_{1-x}$ and $CaCl_2\cdot 6H_2O$.

Fig. 5 shows the density-composition diagram of the quaternary system. It can be seen that on the curve AX_1, BX_1, CX_3, X_1X_2, and DX_3, the density increases with the increase of $J(CaCl_2)$, on EX_2 the density decreases with the increase of $J(CaCl_2)$, while on the curve X_2X_3, the density decreases first and then increases.

3.2. The phase diagram of quaternary system K^+, NH_4^+, Ca^{2+}//Cl^--H_2O at 323.2 K

The experimental data of the quaternary system K^+, NH_4^+, Ca^{2+}//Cl^--H_2O at 323.2 K was listed in Table 4, and the corresponding phase diagram was shown in Fig. 6.

As shown in Fig. 6, the system is a complex system composed of hydrate salt, double salt and solid solution. The system consists of five invariant points (Y_1–Y_5), eleven univariate curves and seven crystallization phase regions, which are $(KCl)_x(NH_4Cl)_{1-x}$, NH_4Cl, KCl, $(NH_4Cl)_x(KCl)_{1-x}$, $2NH_4Cl\cdot CaCl_2\cdot 3H_2O$, $CaCl_2\cdot 2H_2O$, and $KCl\cdot CaCl_2$, and the crystalline phase regions decrease in turn.

The equilibrium solid phases of five invariant points were identified by X-ray, and the corresponding XRD diffraction were shown in Figs. 7–11. And the solid liquid compositions of these five invariant points are as follows:

The solid phase of Y_1 (Fig. 7) is NH_4Cl, $(NH_4Cl)_x(KCl)_{1-x}$, and $(KCl)_x(NH_4Cl)_{1-x}$, and corresponding liquid phase composition is $w(KCl) = 5.88\%$, $w(NH_4Cl) = 14.57\%$, $w(CaCl_2) = 17.84\%$, $w(H_2O) = 61.71\%$. The solid phase of Y_2 (Fig. 8) is NH_4Cl, $(KCl)_x(NH_4Cl)_{1-x}$ and $2NH_4Cl\cdot CaCl_2\cdot 3H_2O$, and corresponding liquid phase composition is $w(KCl) = 3.57\%$, $w(NH_4Cl) = 7.47\%$, $w(CaCl_2) = 40.84\%$, $w(H_2O) = 48.11\%$. The solid phase of Y_3 (Fig. 9) is $(KCl)_x(NH_4Cl)_{1-x}$, $2NH_4Cl\cdot CaCl_2\cdot 3H_2O$, and KCl, and corresponding liquid phase composition is $w(KCl) = 6.77\%$, $w(NH_4Cl) = 3.16\%$, $w(CaCl_2) = 47.64\%$, $w(H_2O) = 42.43\%$. The solid phase of Y_4 (Fig. 10) is $KCl\cdot CaCl_2$, $2NH_4Cl\cdot CaCl_2\cdot 3H_2O$, and KCl, and corresponding liquid phase composition is $w(KCl) = 7.68\%$, $w(NH_4Cl) = 2.31\%$, $w(CaCl_2) = 48.42\%$, $w(H_2O) = 41.59\%$. The solid phase of Y_5 (Fig. 11) is $2NH_4Cl\cdot CaCl_2\cdot 3H_2O$, $CaCl_2\cdot 2H_2O$, and $KCl\cdot CaCl_2$, and corresponding liquid phase composition is $w(KCl) = 4.45\%$, $w(NH_4Cl) = 4.36\%$, $w(CaCl_2) = 50.43\%$, $w(H_2O) = 40.76\%$.

The eleven univariate curves and their corresponding solid phases. FY_1: NH_4Cl+$(NH_4Cl)_x(KCl)_{1-x}$; GY_1: $(NH_4Cl)_x(KCl)_{1-x}$+$(KCl)_x(NH_4Cl)_{1-x}$; Y_1Y_2: NH_4Cl+$(KCl)_x(NH_4Cl)_{1-x}$; LY_2: $2NH_4Cl\cdot CaCl_2\cdot 3H_2O$ + NH_4Cl; Y_2Y_3: $2NH_4Cl\cdot CaCl_2\cdot 3H_2O$+$(KCl)_x(NH_4Cl)_{1-x}$; HY_3:

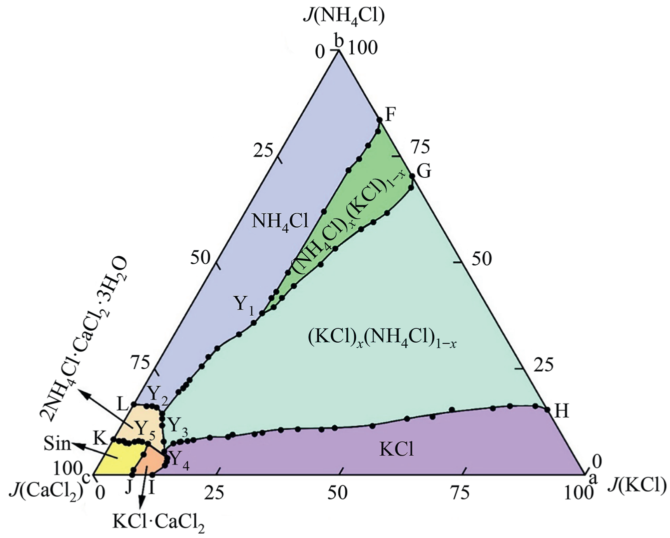

Fig. 6. Phase diagram of quaternary system K^+, NH_4^+, Ca^{2+}//Cl^--H_2O 323.2 K. (Sin: $CaCl_2\cdot 2H_2O$, NCC: $2NH_4Cl\cdot CaCl_2\cdot 3H_2O$).

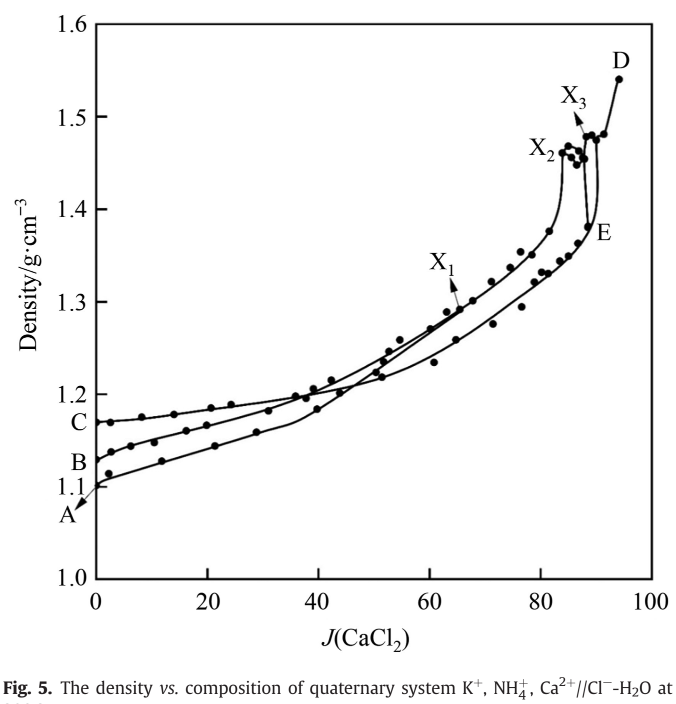

Fig. 5. The density *vs.* composition of quaternary system K^+, NH_4^+, Ca^{2+}//Cl^--H_2O at 298.2 K.

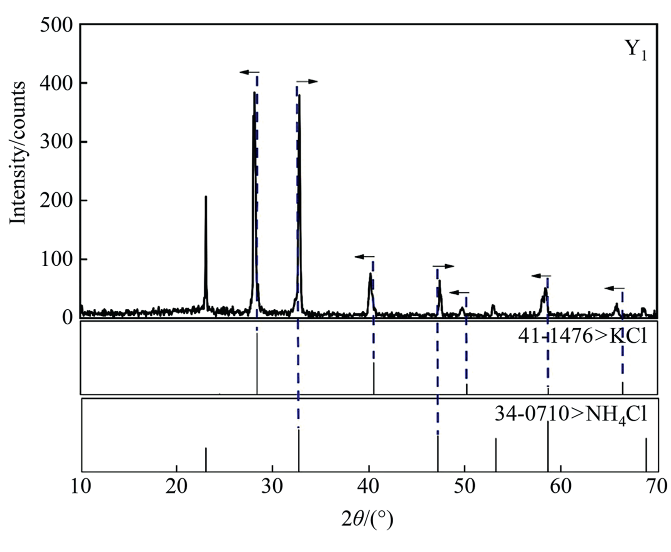

Fig. 7. The XRD pattern of the invariant point Y_1.

Table 4
The experimental date (solubilities, density) of solid-liquid equilibria of the quaternary system K^+, NH_4^+, Ca^{2+}//Cl^--H_2O at 323.2 K

No.	Density, ρ/g·cm^{-3}	Equilibrium solutions composition, w(B)/%				Jänecke index of dry salt, J(B) (g/100 g S)/g·g^{-1}				Equilibrium solid phase (Sal: NH_4Cl, Sin: $CaCl_2\cdot6H_2O$, Chle: $KCl\cdot CaCl_2$)
						$J(KCl)+J(NH_4Cl)+J(CaCl_2)=100$				
		$w(KCl)$	$w(NH_4Cl)$	$w(CaCl_2)$	$w(H_2O)$	$J(KCl)$	$J(NH_4Cl)$	$J(CaCl_2)$	$J(H_2O)$	
1, F	1.1113	5.85	29.74	0.00	64.41	16.44	83.56	0.00	180.98	Sal+$(NH_4Cl)_x(KCl)_{1-x}$
2	1.1078	6.30	29.11	0.59	64.00	17.51	80.85	1.65	177.76	Sal+$(NH_4Cl)_x(KCl)_{1-x}$
3	1.1097	6.18	27.91	1.92	64.00	17.16	77.51	5.33	177.75	Sal+$(NH_4Cl)_x(KCl)_{1-x}$
4	1.1196	6.11	26.83	3.14	63.92	16.93	74.36	8.71	177.16	Sal+$(NH_4Cl)_x(KCl)_{1-x}$
5	1.1287	5.78	25.77	4.40	64.06	16.07	71.68	12.25	178.22	Sal+$(NH_4Cl)_x(KCl)_{1-x}$
6	1.1855	5.76	22.35	7.96	63.93	15.96	61.97	22.07	177.24	Sal+$(NH_4Cl)_x(KCl)_{1-x}$
7	1.2057	5.93	17.84	13.69	62.55	15.82	47.62	36.55	167.00	Sal+$(NH_4Cl)_x(KCl)_{1-x}$
8	1.2144	5.97	16.38	15.64	62.01	15.71	43.11	41.18	163.16	Sal+$(NH_4Cl)_x(KCl)_{1-x}$
9	1.2255	5.92	15.93	16.41	61.73	15.47	41.64	42.89	160.86	Sal+$(NH_4Cl)_x(KCl)_{1-x}$
10, Y_1	1.2580	5.88	14.57	17.84	61.71	15.36	38.05	46.59	161.14	Sal+$(NH_4Cl)_x(KCl)_{1-x}$+$(KCl)_x(NH_4Cl)_{1-x}$
11, G	1.1376	11.05	26.16	0.00	62.79	29.70	70.30	0.00	168.74	$(NH_4Cl)_x(KCl)_{1-x}$+$(KCl)_x(NH_4Cl)_{1-x}$
12	1.1379	11.61	25.45	0.58	62.36	30.84	67.62	1.54	165.68	$(NH_4Cl)_x(KCl)_{1-x}$+$(KCl)_x(NH_4Cl)_{1-x}$
13	1.1372	10.89	23.17	3.54	62.41	28.96	61.63	9.41	166.04	$(NH_4Cl)_x(KCl)_{1-x}$+$(KCl)_x(NH_4Cl)_{1-x}$
14	1.1473	10.26	22.40	5.00	62.33	27.25	59.48	13.28	165.47	$(NH_4Cl)_x(KCl)_{1-x}$+$(KCl)_x(NH_4Cl)_{1-x}$
15	1.1752	9.67	21.86	6.28	62.18	25.58	57.82	16.60	164.44	$(NH_4Cl)_x(KCl)_{1-x}$+$(KCl)_x(NH_4Cl)_{1-x}$
16	1.2051	8.68	20.45	9.27	61.61	22.61	53.26	24.14	160.47	$(NH_4Cl)_x(KCl)_{1-x}$+$(KCl)_x(NH_4Cl)_{1-x}$
17	1.2178	8.12	18.69	10.92	62.27	21.52	49.54	28.94	165.04	$(NH_4Cl)_x(KCl)_{1-x}$+$(KCl)_x(NH_4Cl)_{1-x}$
18	1.2363	7.01	16.76	13.93	62.30	18.60	44.46	36.94	165.23	$(NH_4Cl)_x(KCl)_{1-x}$+$(KCl)_x(NH_4Cl)_{1-x}$
19	1.2413	6.76	16.06	15.70	61.48	17.56	41.70	40.74	159.58	$(NH_4Cl)_x(KCl)_{1-x}$+$(KCl)_x(NH_4Cl)_{1-x}$
20	1.2475	6.51	15.11	16.67	61.71	16.99	39.47	43.54	161.18	$(NH_4Cl)_x(KCl)_{1-x}$+$(KCl)_x(NH_4Cl)_{1-x}$
21	1.2593	5.90	14.28	19.72	60.10	14.78	35.80	49.42	150.64	Sal+$(KCl)_x(NH_4Cl)_{1-x}$
22	1.2728	5.16	13.02	21.18	60.64	13.12	33.08	53.80	154.05	Sal+$(KCl)_x(NH_4Cl)_{1-x}$
23	1.2841	4.09	11.77	23.64	60.51	10.35	29.80	59.85	153.21	Sal+$(KCl)_x(NH_4Cl)_{1-x}$
24	1.2956	3.84	11.17	25.20	59.79	9.56	27.78	62.66	148.67	Sal+$(KCl)_x(NH_4Cl)_{1-x}$
25	1.2950	3.86	10.59	26.96	58.58	9.33	25.56	65.11	141.45	Sal+$(KCl)_x(NH_4Cl)_{1-x}$
26	1.3336	3.68	9.70	30.08	56.54	8.47	22.32	69.21	130.08	Sal+$(KCl)_x(NH_4Cl)_{1-x}$
27	1.5237	7.83	1.82	48.58	41.77	13.44	3.12	83.43	71.73	Sal+$(KCl)_x(NH_4Cl)_{1-x}$
28	1.3440	3.60	9.04	31.66	55.70	8.13	20.40	71.47	125.73	Sal+$(KCl)_x(NH_4Cl)_{1-x}$
29	1.3495	3.43	8.76	32.73	55.08	7.64	19.50	72.86	122.60	Sal+$(KCl)_x(NH_4Cl)_{1-x}$
30, Y_2	1.4407	3.57	7.47	40.84	48.11	6.89	14.39	78.72	92.73	Sal+$(KCl)_x(NH_4Cl)_{1-x}$+$2NH_4Cl\cdot CaCl_2\cdot3H_2O$
31, H	1.1771	26.08	4.72	0.00	69.20	84.68	15.32	0.00	224.68	$(KCl)_x(NH_4Cl)_{1-x}$ + KCl
32	1.1846	25.19	4.99	0.61	69.21	81.81	16.20	2.00	224.76	$(KCl)_x(NH_4Cl)_{1-x}$ + KCl
33	1.1732	23.33	4.93	2.18	69.56	76.64	16.21	7.15	228.51	$(KCl)_x(NH_4Cl)_{1-x}$ + KCl
34	1.1953	22.66	4.83	3.36	69.15	73.45	15.67	10.89	224.17	$(KCl)_x(NH_4Cl)_{1-x}$ + KCl
35	1.1929	19.93	4.68	5.92	69.47	65.27	15.33	19.40	227.58	$(KCl)_x(NH_4Cl)_{1-x}$ + KCl
36	1.2064	19.28	4.24	7.48	68.99	62.19	13.68	24.13	222.52	$(KCl)_x(NH_4Cl)_{1-x}$ + KCl
37	1.2217	18.28	4.21	9.44	68.06	57.26	13.20	29.55	213.13	$(KCl)_x(NH_4Cl)_{1-x}$ + KCl
38	1.2272	16.13	3.64	11.84	68.39	51.04	11.50	37.46	216.37	$(KCl)_x(NH_4Cl)_{1-x}$ + KCl
39	1.2430	13.97	3.53	14.52	67.98	43.63	11.03	45.35	212.35	$(KCl)_x(NH_4Cl)_{1-x}$ + KCl
40	1.2430	13.37	3.47	15.66	67.49	41.13	10.69	48.19	207.64	$(KCl)_x(NH_4Cl)_{1-x}$ + KCl
41	1.2541	11.90	3.53	17.38	67.19	36.26	10.76	52.99	204.80	$(KCl)_x(NH_4Cl)_{1-x}$ + KCl
42	1.2721	10.94	3.51	18.80	66.75	32.91	10.56	56.53	200.75	$(KCl)_x(NH_4Cl)_{1-x}$ + KCl
43	1.2792	10.11	3.40	20.80	65.68	29.47	9.92	60.62	191.39	$(KCl)_x(NH_4Cl)_{1-x}$ + KCl
44	1.2860	9.82	3.36	21.84	64.98	28.04	9.60	62.36	185.56	$(KCl)_x(NH_4Cl)_{1-x}$ + KCl
45	1.2872	8.33	3.33	23.55	64.79	23.65	9.46	66.88	184.03	$(KCl)_x(NH_4Cl)_{1-x}$ + KCl
46	1.2944	8.17	3.17	24.16	64.50	23.01	8.93	68.06	181.71	$(KCl)_x(NH_4Cl)_{1-x}$ + KCl
47	1.3017	6.93	3.14	25.74	64.18	19.35	8.77	71.88	179.19	$(KCl)_x(NH_4Cl)_{1-x}$ + KCl
48	1.3119	6.33	3.18	29.29	61.21	16.31	8.19	75.49	157.77	$(KCl)_x(NH_4Cl)_{1-x}$ + KCl
49	1.3215	5.73	3.00	28.89	62.38	15.24	7.97	76.79	165.79	$(KCl)_x(NH_4Cl)_{1-x}$ + KCl
50	1.3262	5.25	2.94	29.41	62.40	13.97	7.82	78.20	165.94	$(KCl)_x(NH_4Cl)_{1-x}$ + KCl
51	1.3354	5.02	2.94	31.76	60.28	12.65	7.40	79.95	151.76	$(KCl)_x(NH_4Cl)_{1-x}$ + KCl
52, Y_3	1.5526	6.77	3.16	47.64	42.43	11.76	5.50	82.74	73.69	$(KCl)_x(NH_4Cl)_{1-x}$ + KCl+$2NH_4Cl\cdot CaCl_2\cdot3H_2O$
53, L	1.4068	0.00	8.52	42.74	48.74	0.00	16.62	83.38	95.08	Sal+$2NH_4Cl\cdot CaCl_2\cdot3H_2O$
54	1.4263	1.43	8.22	41.18	49.16	2.82	16.17	81.01	96.70	Sal+$2NH_4Cl\cdot CaCl_2\cdot3H_2O$
55	1.4423	2.02	8.34	41.10	48.54	3.92	16.20	79.87	94.34	Sal+$2NH_4Cl\cdot CaCl_2\cdot3H_2O$
56	1.4270	2.58	8.20	40.83	48.40	5.00	15.88	79.12	93.80	Sal+$2NH_4Cl\cdot CaCl_2\cdot3H_2O$
57	1.4446	3.92	6.95	41.63	47.51	7.46	13.23	79.31	90.50	$(KCl)_x(NH_4Cl)_{1-x}$+$2NH_4Cl\cdot CaCl_2\cdot3H_2O$
58	1.4993	4.69	6.64	45.70	42.98	8.22	11.64	80.14	75.37	$(KCl)_x(NH_4Cl)_{1-x}$+$2NH_4Cl\cdot CaCl_2\cdot3H_2O$
59	1.5375	6.10	4.57	47.59	41.74	10.47	7.84	81.69	71.66	$(KCl)_x(NH_4Cl)_{1-x}$+$2NH_4Cl\cdot CaCl_2\cdot3H_2O$
60	1.5344	7.02	3.04	47.58	42.36	12.18	5.27	82.55	73.50	$2NH_4Cl\cdot CaCl_2\cdot3H_2O$ + KCl
61, Y_4	1.5494	7.68	2.31	48.42	41.59	13.16	3.95	82.89	71.20	$2NH_4Cl\cdot CaCl_2\cdot3H_2O$ + KCl + Chle
62, J	1.6655	4.63	0.00	53.36	42.02	7.98	0.00	92.02	72.47	Sin + Chle
63	1.6732	4.52	0.69	53.89	40.90	7.64	1.17	91.18	69.19	Sin + Chle
64	1.6552	4.76	2.90	52.70	39.65	7.88	4.80	87.32	65.70	Sin + Chle
65, Y_5	1.6299	4.45	4.36	50.43	40.76	7.51	7.36	85.13	68.82	Sin + Chle+$2NH_4Cl\cdot CaCl_2\cdot3H_2O$
66. K	1.5417	0.00	4.81	52.82	42.37	0.00	8.35	91.65	73.52	Sin+$2NH_4Cl\cdot CaCl_2\cdot3H_2O$
67	1.5072	0.78	4.80	54.60	39.82	1.30	7.97	90.73	66.16	Sin+$2NH_4Cl\cdot CaCl_2\cdot3H_2O$
68	1.5291	1.34	4.84	54.31	39.51	2.21	8.01	89.78	65.33	Sin+$2NH_4Cl\cdot CaCl_2\cdot3H_2O$
69	1.5256	1.79	4.65	55.33	38.22	2.90	7.53	89.57	61.88	Sin+$2NH_4Cl\cdot CaCl_2\cdot3H_2O$
70	1.5291	2.19	4.53	54.22	39.06	3.60	7.43	88.97	64.11	Sin+$2NH_4Cl\cdot CaCl_2\cdot3H_2O$
71	1.5297	2.83	4.83	54.35	37.98	4.57	7.79	87.64	61.25	Sin+$2NH_4Cl\cdot CaCl_2\cdot3H_2O$

(continued on next page)

Table 4 (*continued*)

No.	Density, ρ/g·cm^{-3}	Equilibrium solutions composition, w(B)/%				Jänecke index of dry salt, J(B) (g/100 g S)/g·g^{-1} $J(KCl)+J(NH_4Cl)+J(CaCl_2)=100$				Equilibrium solid phase (Sal: NH_4Cl, Sin: $CaCl_2\cdot 6H_2O$, Chle: $KCl\cdot CaCl_2$)
		w(KCl)	$w(NH_4Cl)$	$w(CaCl_2)$	$w(H_2O)$	J(KCl)	$J(NH_4Cl)$	$J(CaCl_2)$	$J(H_2O)$	
72	1.5207	3.12	4.73	51.30	40.86	5.28	7.99	86.73	69.08	Sin+$2NH_4Cl\cdot CaCl_2\cdot 3H_2O$
73	1.5334	3.65	4.66	51.51	40.18	6.10	7.79	86.11	67.16	Sin+$2NH_4Cl\cdot CaCl_2\cdot 3H_2O$
74	1.5237	7.83	1.82	48.58	41.77	13.44	3.12	83.43	71.73	Chle + KCl
75	1.5306	7.84	1.28	48.89	41.98	13.52	2.21	84.27	72.35	Chle + KCl
76, I	1.5716	7.24	0.00	52.74	40.02	12.07	0.00	87.93	66.72	Chle + KCl

Note: Standard uncertainties u are $u(T) = 0.20$ K, $u(\rho) = 0.0002$ g·cm^{-3}; the relative standard uncertainties u_r are $u_r(w(KCl)) = 0.0030$, $u_r(w(NH_4Cl)) = 0.0031$, and $u_r(w(CaCl_2)) = 0.0046$.

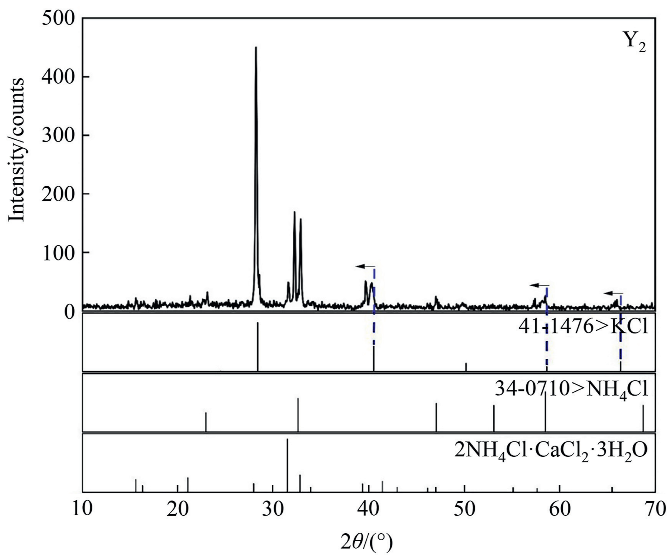

Fig. 8. The XRD pattern of the invariant point Y_2.

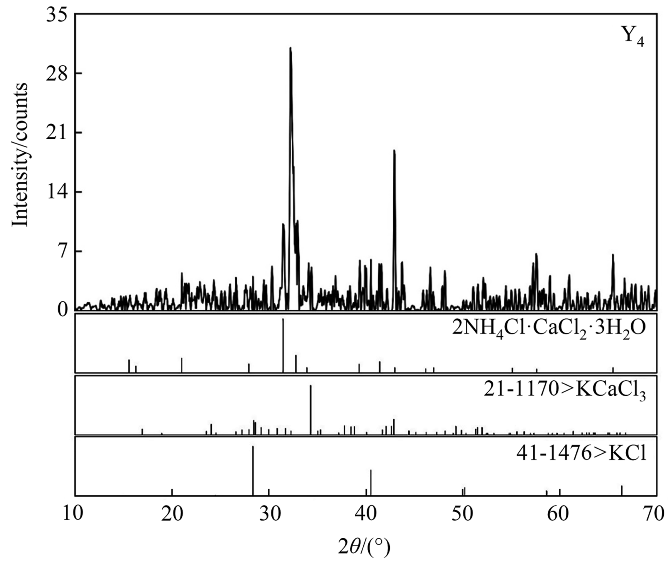

Fig. 10. The XRD pattern of the invariant point Y_4.

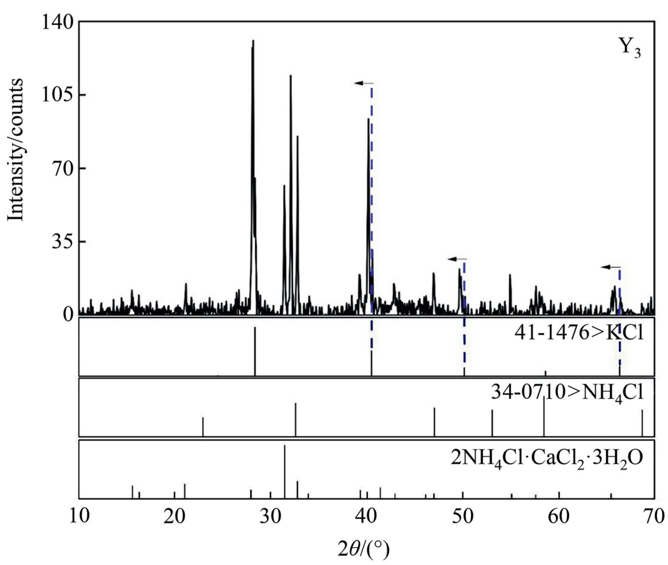

Fig. 9. The XRD pattern of the invariant point Y_3.

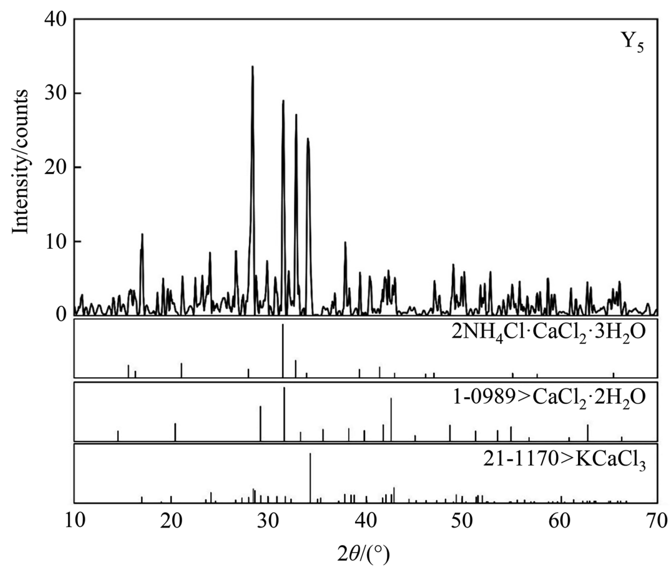

Fig. 11. The XRD pattern of the invariant point Y_5.

$(KCl)_x(NH_4Cl)_{1-x}$ + KCl; Y_3Y_4: $2NH_4Cl\cdot CaCl_2\cdot 3H_2O$ + KCl; Y_4I: KCl + $KCl\cdot CaCl_2$; Y_4Y_5: $KCl\cdot CaCl_2$+$2NH_4Cl\cdot CaCl_2\cdot 3H_2O$; KY_5: $2NH_4Cl\cdot CaCl_2\cdot 3H_2O$ + $CaCl_2\cdot 2H_2O$; JY_5: $CaCl_2\cdot 2H_2O$ + $KCl\cdot CaCl_2$.

Fig. 12 shows the density-composition diagram of the system at 323.2 K. It can be seen that on the curve LY_2, the density decreases with the increase of $J(CaCl_2)$, while on the curve KY_5, the density decreases first and then increases. The other curves increase with the increase of $J(CaCl_2)$.

3.3. The phase diagram of quaternary system K^+, NH_4^+, Ca^{2+}//Cl^--H_2O at 348.2 K

The experimental data of the quaternary system was listed in Table 5, and the equilibrium phase diagram was shown in Fig. 13.

From Fig. 13, it showed that compared with 323.2 K, there is no new salt formation at 348.2 K, and the composition of the phase diagram does not change. It is still composed of five invariant points (Z_1–Z_5), eleven univariate curves and seven crystallization phase regions. The crystalline phase regions decrease in the order of $(KCl)_x(NH_4Cl)_{1-x}$, KCl, NH_4Cl, $(NH_4Cl)_x(KCl)_{1-x}$, $2NH_4Cl\cdot CaCl_2\cdot 3H_2O$, $KCl\cdot CaCl_2$, and $CaCl_2\cdot 2H_2O$.

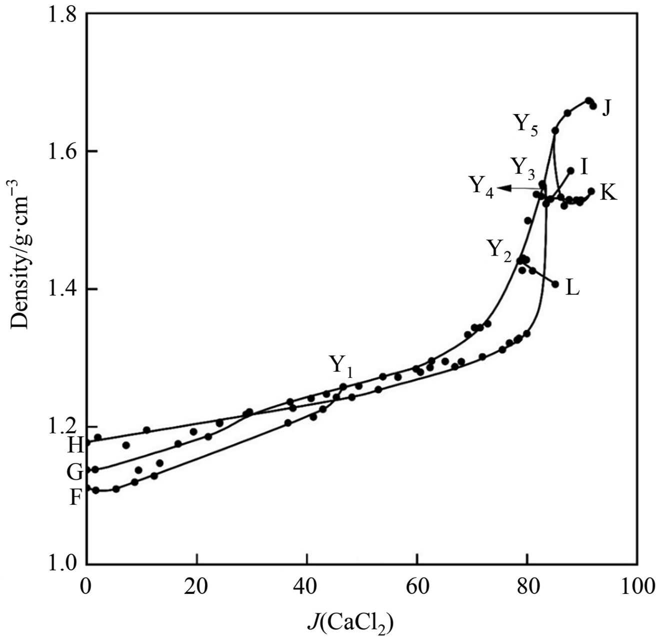

Fig. 12. The density *vs.* composition of the quaternary system K^+, NH_4^+, Ca^{2+}//Cl^--H_2O at 323.2 K.

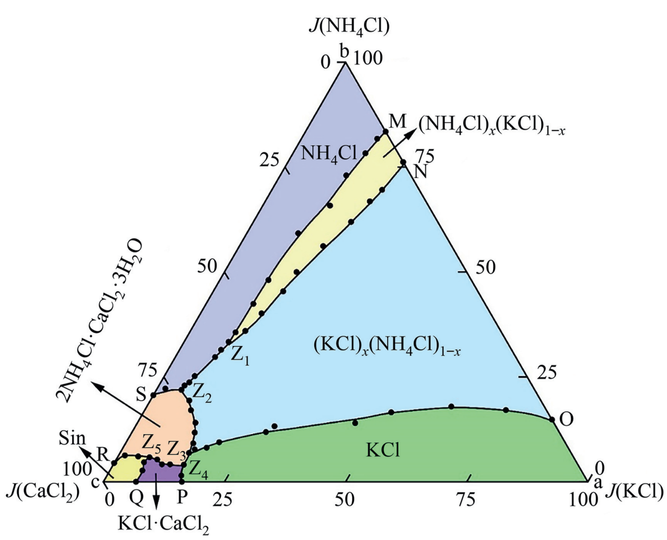

Fig. 13. Phase diagram of quaternary system K^+, NH_4^+, Ca^{2+}//Cl^--H_2O 348.2 K. (Sin: $CaCl_2\cdot 2H_2O$).

The equilibrium solid phases of five invariant points were identified by X-ray, and the corresponding XRD diffraction were shown in Figs. 14–18. And the solid phase compositions of these five invariant points is the same as that at 323.2 K, the liquid phase compositions are as follows:

The liquid phase of Z_1 (Fig. 14) composition is $w(KCl) = 4.29\%$, $w(NH_4Cl) = 15.51\%$, $w(CaCl_2) = 26.75\%$, $w(H_2O) = 53.44\%$. The equilibrium liquid phase of Z_2 (Fig. 15) is $w(KCl) = 2.91\%$, $w(NH_4Cl) = 12.29\%$, $w(CaCl_2) = 40.91\%$, $w(H_2O) = 43.89\%$. The equilibrium liquid phase of Z_3 (Fig. 16) is $w(KCl) = 8.36\%$, $w(NH_4Cl) = 4.04\%$, $w(CaCl_2) = 46.24\%$, $w(H_2O) = 41.37\%$. The equilibrium liquid phase of Z_4 (Fig. 17) is $w(KCl) = 8.87\%$, $w(NH_4Cl) = 2.47\%$, $w(CaCl_2) = 49.43\%$, $w(H_2O) = 39.24\%$. The equilibrium liquid phase of Z_5 (Fig. 18) is $w(KCl) = 3.97\%$, $w(NH_4Cl) = 3.50\%$, $w(CaCl_2) = 52.61\%$, $w(H_2O) = 39.92\%$.

Fig. 19 shows the density-composition diagram of the quaternary system. It can be seen that on the curve MZ_1, NZ_1, OZ_3, Z_1Z_2, Z_2Z_3, Z_3Z_4, and QZ_5 the density increases with the increase of $J(CaCl_2)$, on SZ_2 and PZ_4 the density decreases with the increase of $J(CaCl_2)$, while on the curve Z_4Z_5 and RZ_5, the density decreases first and then increases.

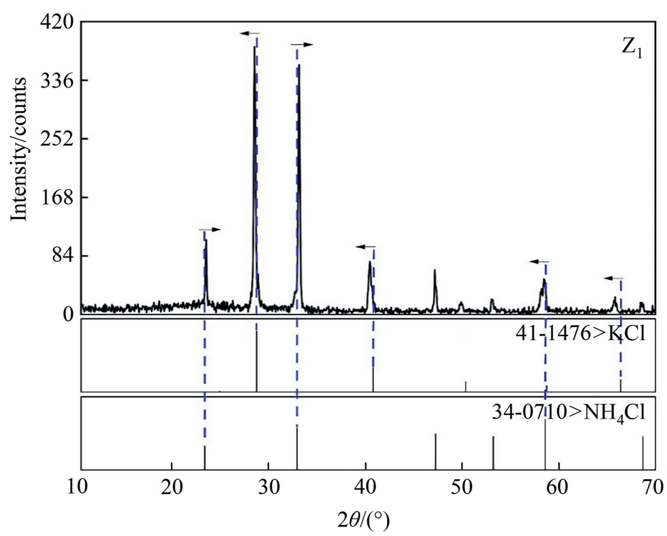

Fig. 14. The XRD pattern of the invariant point Z_1.

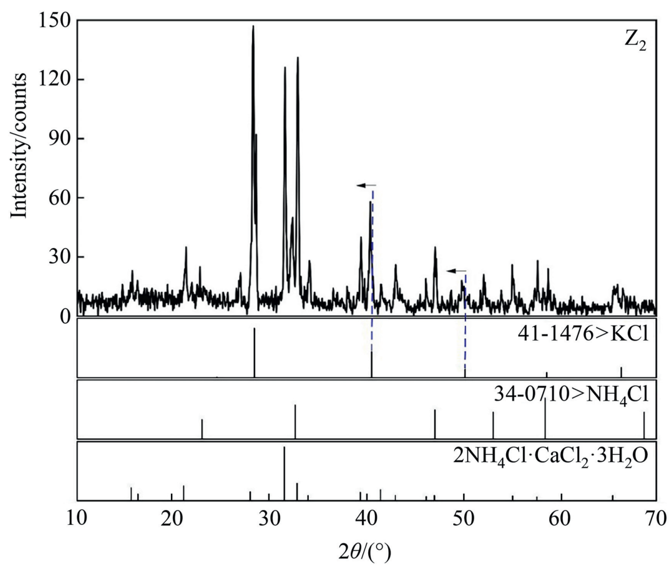

Fig. 15. The XRD pattern of the invariant point Z_2.

Table 5
The experimental date (solubilities, density) of solid–liquid equilibria of the quaternary system K^+, NH_4^+, $Ca^{2+}//Cl^-$-H_2O at 348.2 K

No.	Density, ρ/g·cm^{-3}	Equilibrium solutions composition, w(B)/%				Jänecke index of dry salt, J(B) (g/100 g S)/g·g^{-1} $J(KCl)+J(NH_4Cl)+J(CaCl_2)=100$				Equilibrium solid phase (Sal: NH_4Cl, Sin: $CaCl_2\cdot 6H_2O$, Chle: $KCl\cdot CaCl_2$)
		$w(KCl)$	$w(NH_4Cl)$	$w(CaCl_2)$	$w(H_2O)$	$J(KCl)$	$J(NH_4Cl)$	$J(CaCl_2)$	$J(H_2O)$	
1, M	1.2141	6.88	34.68	0.00	58.44	16.55	83.45	0.00	140.62	Sal+$(NH_4Cl)_x(KCl)_{1-x}$
2	1.2102	6.43	33.57	1.06	58.94	15.67	81.76	2.57	143.52	Sal+$(NH_4Cl)_x(KCl)_{1-x}$
3	1.2396	6.12	32.02	2.77	59.09	14.96	78.28	6.76	144.47	Sal+$(NH_4Cl)_x(KCl)_{1-x}$
4	1.2472	5.68	30.33	5.54	58.45	13.66	73.00	13.34	140.67	Sal+$(NH_4Cl)_x(KCl)_{1-x}$
5	1.2695	5.73	27.17	8.38	58.73	13.88	65.82	20.30	142.29	Sal+$(NH_4Cl)_x(KCl)_{1-x}$
6	1.3168	4.45	24.82	12.65	58.08	10.62	59.21	30.17	138.56	Sal+$(NH_4Cl)_x(KCl)_{1-x}$
7	1.3380	4.35	20.83	18.13	56.68	10.05	48.10	41.86	130.85	Sal+$(NH_4Cl)_x(KCl)_{1-x}$
8	1.3744	4.38	18.98	21.40	55.24	9.78	42.41	47.81	123.40	Sal+$(NH_4Cl)_x(KCl)_{1-x}$
9	1.4080	4.34	16.29	25.08	54.29	9.50	35.63	54.87	118.76	Sal+$(NH_4Cl)_x(KCl)_{1-x}$
10, Z_1	1.4246	4.29	15.51	26.75	53.44	9.22	33.32	57.46	114.79	Sal+$(NH_4Cl)_x(KCl)_{1-x}$+$(KCl)_x(NH_4Cl)_{1-x}$
11, N	1.2313	10.15	32.47	0.00	57.38	23.82	76.18	0.00	134.63	$(NH_4Cl)_x(KCl)_{1-x}$+$(KCl)_x(NH_4Cl)_{1-x}$
12	1.2464	9.60	29.32	3.23	57.85	22.77	69.57	7.66	137.27	$(NH_4Cl)_x(KCl)_{1-x}$+$(KCl)_x(NH_4Cl)_{1-x}$
13	1.2610	9.06	28.01	4.84	58.09	21.62	66.84	11.54	138.59	$(NH_4Cl)_x(KCl)_{1-x}$+$(KCl)_x(NH_4Cl)_{1-x}$
14	1.2709	8.41	25.81	7.45	58.33	20.19	61.93	17.88	139.98	$(NH_4Cl)_x(KCl)_{1-x}$+$(KCl)_x(NH_4Cl)_{1-x}$
15	1.2832	7.35	23.84	11.26	57.56	17.31	56.17	26.52	135.63	$(NH_4Cl)_x(KCl)_{1-x}$+$(KCl)_x(NH_4Cl)_{1-x}$
16	1.3020	6.35	21.29	14.96	57.41	14.90	49.98	35.12	134.79	$(NH_4Cl)_x(KCl)_{1-x}$+$(KCl)_x(NH_4Cl)_{1-x}$
17	1.3456	6.30	19.81	17.55	56.34	14.43	45.38	40.19	129.04	$(NH_4Cl)_x(KCl)_{1-x}$+$(KCl)_x(NH_4Cl)_{1-x}$
18	1.3727	5.63	17.88	21.07	55.42	12.62	40.11	47.27	124.31	$(NH_4Cl)_x(KCl)_{1-x}$+$(KCl)_x(NH_4Cl)_{1-x}$
19	1.3930	5.14	16.33	23.95	54.58	11.32	35.95	52.72	120.16	$(NH_4Cl)_x(KCl)_{1-x}$+$(KCl)_x(NH_4Cl)_{1-x}$
20	1.4433	4.03	14.71	28.07	53.19	8.60	31.43	59.97	113.63	Sal+$(KCl)_x(NH_4Cl)_{1-x}$
21	1.4572	3.93	14.22	29.69	52.16	8.21	29.72	62.07	109.04	Sal+$(KCl)_x(NH_4Cl)_{1-x}$
22	1.4918	3.13	12.57	34.21	50.09	6.28	25.18	68.54	100.35	Sal+$(KCl)_x(NH_4Cl)_{1-x}$
23	1.5229	3.02	12.11	35.99	48.89	5.90	23.69	70.41	95.66	Sal+$(KCl)_x(NH_4Cl)_{1-x}$
24	1.5414	2.80	12.08	37.77	47.36	5.31	22.94	71.75	89.97	Sal+$(KCl)_x(NH_4Cl)_{1-x}$
25, Z_2	1.5822	2.91	12.29	40.91	43.89	5.18	21.91	72.91	78.24	Sal+$(KCl)_x(NH_4Cl)_{1-x}$+$2NH_4Cl\cdot CaCl_2\cdot 3H_2O$
26, O	1.2884	29.55	5.13	0.00	65.32	85.21	14.79	0.00	188.35	$(KCl)_x(NH_4Cl)_{1-x}$ + KCl
27	1.2948	25.86	5.93	2.90	65.31	74.55	17.10	8.35	188.24	$(KCl)_x(NH_4Cl)_{1-x}$ + KCl
28	1.3324	22.14	6.31	6.76	64.79	62.89	17.91	19.20	184.01	$(KCl)_x(NH_4Cl)_{1-x}$ + KCl
29	1.3462	18.26	5.91	11.52	64.31	51.16	16.55	32.29	180.19	$(KCl)_x(NH_4Cl)_{1-x}$ + KCl
30	1.3624	16.28	5.06	14.84	63.83	45.01	13.98	41.02	176.48	$(KCl)_x(NH_4Cl)_{1-x}$ + KCl
31	1.3856	10.89	5.02	22.03	62.06	28.70	13.24	58.05	163.56	$(KCl)_x(NH_4Cl)_{1-x}$ + KCl
32	1.4181	10.54	4.52	23.08	61.86	27.64	11.84	60.52	162.18	$(KCl)_x(NH_4Cl)_{1-x}$ + KCl
33	1.4501	7.94	3.90	29.52	58.64	19.20	9.42	71.38	141.80	$(KCl)_x(NH_4Cl)_{1-x}$ + KCl
34	1.4819	7.34	3.45	31.67	57.55	17.29	8.12	74.60	135.57	$(KCl)_x(NH_4Cl)_{1-x}$ + KCl
35	1.5099	6.78	3.48	34.85	54.90	15.02	7.71	77.26	121.72	$(KCl)_x(NH_4Cl)_{1-x}$ + KCl
36, Z_3	1.6944	8.36	4.04	46.24	41.37	14.26	6.88	78.86	70.55	$(KCl)_x(NH_4Cl)_{1-x}$ + KCl+$2NH_4Cl\cdot CaCl_2\cdot 3H_2O$
37, S	1.5543	0.00	10.86	41.73	47.41	0.00	20.65	79.35	90.15	Sal+$2NH_4Cl\cdot CaCl_2\cdot 3H_2O$
38	1.5784	0.92	11.99	41.09	46.01	1.70	22.20	76.10	85.23	Sal+$2NH_4Cl\cdot CaCl_2\cdot 3H_2O$
39	1.5818	4.33	10.39	38.96	46.32	8.06	19.35	72.59	86.29	$(KCl)_x(NH_4Cl)_{1-x}$+$2NH_4Cl\cdot CaCl_2\cdot 3H_2O$
40	1.6328	5.80	10.32	44.42	39.46	9.58	17.05	73.37	65.18	$(KCl)_x(NH_4Cl)_{1-x}$+$2NH_4Cl\cdot CaCl_2\cdot 3H_2O$
41	1.6884	7.20	8.45	44.43	39.92	11.99	14.06	73.95	66.45	$(KCl)_x(NH_4Cl)_{1-x}$+$2NH_4Cl\cdot CaCl_2\cdot 3H_2O$
42	1.6896	7.71	6.94	44.60	40.75	13.01	11.71	75.28	68.78	$(KCl)_x(NH_4Cl)_{1-x}$+$2NH_4Cl\cdot CaCl_2\cdot 3H_2O$
43	1.6991	8.22	5.37	45.18	41.22	13.99	9.14	76.87	70.13	$(KCl)_x(NH_4Cl)_{1-x}$+$2NH_4Cl\cdot CaCl_2\cdot 3H_2O$
44, Z_4	1.7630	8.87	2.47	49.43	39.24	14.59	4.06	81.34	64.57	$2NH_4Cl\cdot CaCl_2\cdot 3H_2O$ + KCl + Chle
45, Q	1.6459	3.94	0.00	54.41	41.65	6.75	0.00	93.25	71.37	Sin + Chle
46	1.7167	4.03	1.61	54.22	40.14	6.74	2.68	90.58	67.06	Sin + Chle
47	1.6412	3.71	2.84	54.40	39.06	6.08	4.65	89.26	64.09	Sin + Chle
48, Z_5	1.6454	3.97	3.50	52.61	39.92	6.62	5.83	87.56	66.44	Sin + Chle+$2NH_4Cl\cdot CaCl_2\cdot 3H_2O$
49, R	1.7081	0.00	2.63	56.05	41.32	0.00	4.48	95.52	70.42	Sin+$2NH_4Cl\cdot CaCl_2\cdot 3H_2O$
50	1.7404	0.78	3.76	55.23	40.23	1.31	6.29	92.40	67.30	Sin+$2NH_4Cl\cdot CaCl_2\cdot 3H_2O$
51	1.6917	2.36	3.40	50.54	43.70	4.19	6.03	89.78	77.62	Sin+$2NH_4Cl\cdot CaCl_2\cdot 3H_2O$
52	1.7468	5.04	3.15	51.37	40.44	8.47	5.29	86.24	67.89	$2NH_4Cl\cdot CaCl_2\cdot 3H_2O$ + Chle
53	1.7562	6.25	2.58	53.42	37.75	10.04	4.14	85.82	60.65	$2NH_4Cl\cdot CaCl_2\cdot 3H_2O$ + Chle
54	1.7786	7.27	2.57	52.23	37.94	11.71	4.14	84.15	61.13	$2NH_4Cl\cdot CaCl_2\cdot 3H_2O$ + Chle
55	1.7357	9.01	0.87	48.78	41.34	15.35	1.49	83.16	70.48	Chle + KCl
56, P	1.6511	9.36	0.00	48.36	42.28	16.22	0.00	83.78	73.25	Chle + KCl

Note: Standard uncertainties u are $u(T) = 0.20$ K, $u(\rho) = 0.0002$ g cm^{-3}; the relative standard uncertainties u_r are $u_r(w(KCl)) = 0.0030$, $u_r(w(NH_4Cl)) = 0.0031$, and $u_r(w(CaCl_2)) = 0.0046$.

3.4. Comparison of multi-temperature phase diagrams of quaternary system K^+, NH_4^+, $Ca^{2+}//Cl^-$-H_2O

The experimental data of the invariant points of the related ternary sub-systems K^+, $NH_4^+//Cl^-$-H_2O, K^+, $Ca^{2+}//Cl^-$-H_2O, and NH_4^+, $Ca^{2+}//Cl^-$-H_2O are compared with the existing data, as shown in Table 6. It can be found that the deviation between the experimental value and the reference value is related to the coexisting ions in the equilibrium solution. On the whole, the deviation between the experimental data of the invariant point of the ternary sub-system and the existing data is within 2.03%.

In order to analyze the effect of temperature on the solubility of salts and the interaction between ions in the system, a multi-temperature comparison diagram of the system was drawn (Fig. 20). It showed that the configuration of the phase diagram changed at three temperatures. The invariant points, univariate

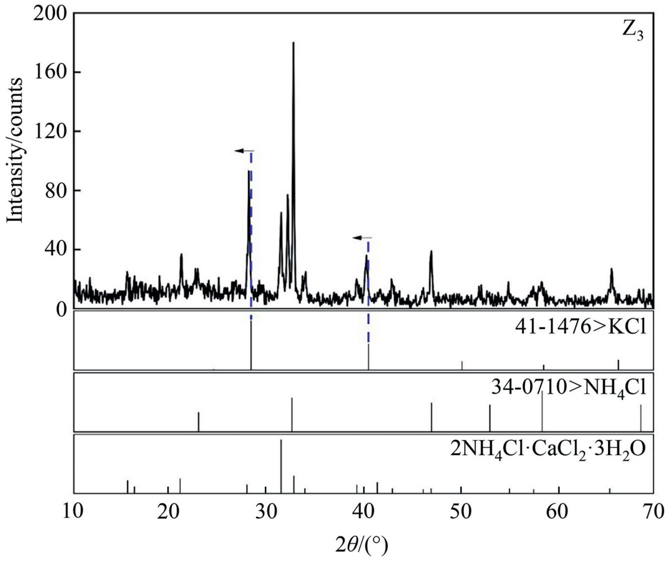

Fig. 16. The XRD pattern of the invariant point Z_3.

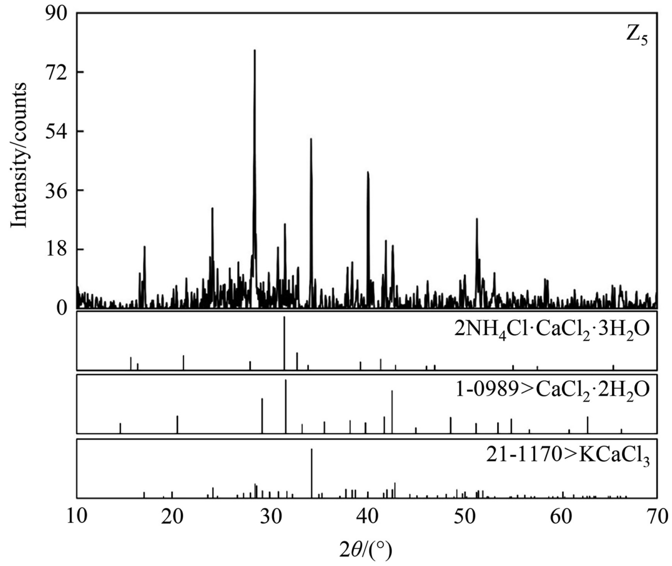

Fig. 18. The XRD pattern of the invariant point Z_5.

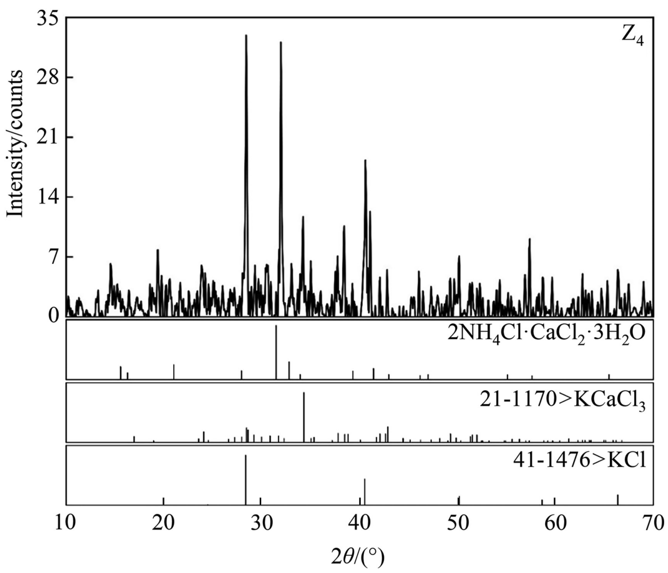

Fig. 17. The XRD pattern of the invariant point Z_4.

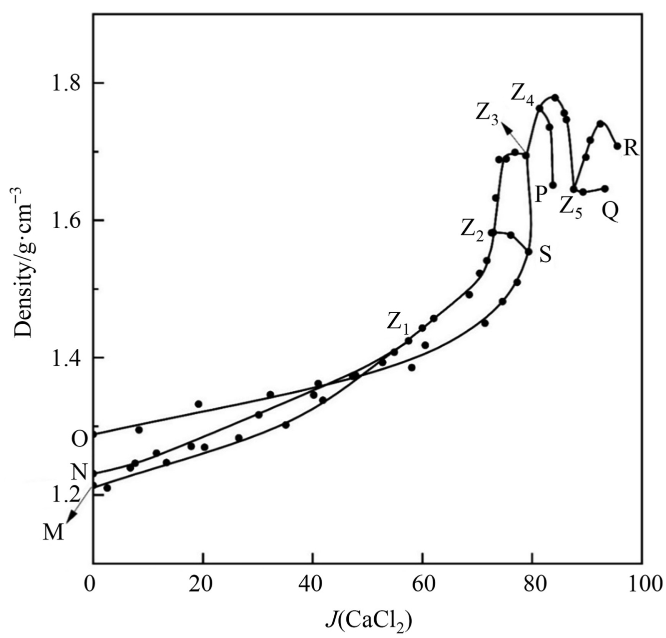

Fig. 19. The density vs composition of the quaternary system K^+, NH_4^+, Ca^{2+}//Cl^--H_2O at 348.2 K.

curves and crystallization regions increased. The fundamental reason is that the double salts $2NH_4Cl\cdot CaCl_2\cdot 3H_2O$ and $KCl\cdot CaCl_2$ are produced at 323.2 and 348.2 K.

The change of temperature caused the change of the crystal form of salt. There is no double salt at 298.2 K, and there is a new salt action relationship at 323.2 and 348.2 K. The double salts ($2NH_4Cl\cdot CaCl_2\cdot 3H_2O$) and ($KCl\cdot CaCl_2$) were formed at these two temperatures, both of the double salts phase regions increase with the increase of temperature. The precipitation form of $CaCl_2$ is $CaCl_2\cdot 6H_2O$ at 298.2 K, and $CaCl_2\cdot 2H_2O$ at 323.2 and 348.2 K, which is consistent with the change of K^+, Ca^{2+}//Cl^--H_2O in the ternary system.

In addition, temperature has an effect on the solubility of each salt, while the sensitivity of each salt to temperature is different. What is shown in the phase diagram is that the crystalline phase regions increase or decrease. The solid solution $(KCl)_x(NH_4Cl)_{1-x}$ is the largest crystalline phase in the system, and the crystalline phase region of the two solid solutions accounts for more than half of the whole phase diagram, which brings great difficulties to the separation and enrichment of KCl. The most obvious change in this system is the crystalline phase region of NH_4Cl, which decreases with the increase of temperature, while KCl is the opposite. It can be seen that high temperature is beneficial to the precipitation of KCl, which is not conducive to the precipitation of NH_4Cl.

According to the content of related ions in the brine of northeast Sichuan, the salt precipitation route is roughly drawn in the multi-temperature phase diagram by calculation, and the specific salt precipitation law is shown in Fig. 20 (b), (c). Due to the saturation of NaCl in the brine, NaCl is the first to precipitate; KCl is saturated at point B, so NaCl + KCl is precipitated. According to the route, $(KCl)_x(NH_4Cl)_{1-x}$ began to precipitate at point C, accompanied by

Table 6
The comparison between experimental data and existing data of subsystems invariant points at 298.2, 323.2, and 348.2 K

System	T/K	Composition of equilibrium liquid phase, w(B)/%				Solid phase	Source
		w(KCl)	w(NH_4Cl)	w($CaCl_2$)	w(H_2O)		
K^+, NH_4^+//Cl^--H_2O	323.2	11.10	25.40	–	63.50	KCl + Sal	[30]
		24.66	6.75	–	68.59	KCl + $(KCl)_x(NH_4Cl)_{1-x}$	[31]
		5.85	29.74	–	64.41	$(NH_4Cl)_x(KCl)_{1-x}$ + Sal	This work
		11.05	26.16	–	62.79	$(NH_4Cl)_x(KCl)_{1-x}$ + $(KCl)_x(NH_4Cl)_{1-x}$	
		26.08	4.72	–	69.20	$(KCl)_x(NH_4Cl)_{1-x}$ + KCl	
K^+, Ca^{2+}//Cl^--H_2O	298.2	2.81	–	45.62	51.57	KCl + Ant	[19]
		2.86	–	45.68	51.46	KCl + Ant	This work
	323.2	4.24	–	55.07	40.69	Sin + Chle	[19]
		7.40	–	51.88	40.72	Chle + KCl	
		4.63	–	53.36	42.02	Sin + Chle	This work
		7.24	–	52.74	40.02	Chle + KCl	
	348.2	3.69	–	56.56	39.75	Sin + Chle	[19]
		9.36	–	48.36	42.38	Chle + KCl	
		3.94	–	54.41	41.65	Sin + Chle	This work
		9.36	–	48.36	42.28	Chle + KCl	
NH_4^+, Ca^{2+}//Cl^--H_2O	348.2	–	2.62	57.67	39.71	Sin + $2NH_4Cl\cdot CaCl_2\cdot 3H_2O$	[31]
		–	10.79	42.34	46.87	Sal + $2NH_4Cl\cdot CaCl_2\cdot 3H_2O$	
		–	2.63	56.05	41.32	Sin + $2NH_4Cl\cdot CaCl_2\cdot 3H_2O$	This work
		–	10.86	41.73	47.41	Sal + $2NH_4Cl\cdot CaCl_2\cdot 3H_2O$	

Note: Sal—NH_4Cl, Ant—$CaCl_2\cdot 6H_2O$, Sin—$CaCl_2\cdot 2H_2O$, Chle—$KCl\cdot CaCl_2$.

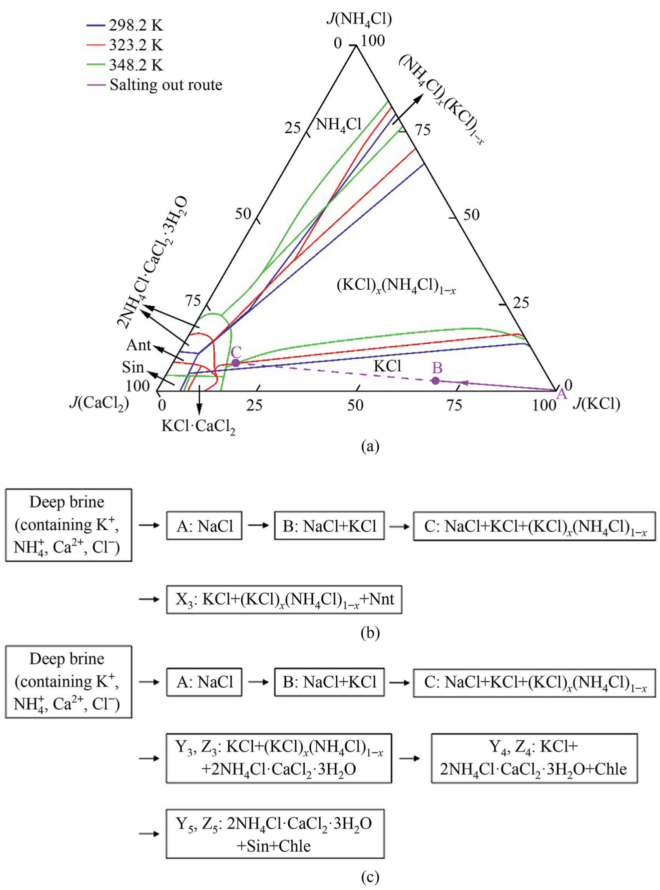

Fig. 20. (a) Phase diagram of the quaternary system K^+, NH_4^+, Ca^{2+}//Cl^--H_2O at 298.2 K, 323.2 K, and 348.2 K. (b) Salt precipitation route of deep brine in the quaternary system K^+, NH_4^+, Ca^{2+}//Cl^--H_2O at 298.2 K. (c) Salt precipitation route of deep brine in the quaternary system K^+, NH_4^+, Ca^{2+}//Cl^--H_2O at 323.2 and 348.2 K. (Ant: $CaCl_2\cdot 6H_2O$, Sin: $CaCl_2\cdot 2H_2O$, Chle: $KCl\cdot CaCl_2$).

the precipitation of NaCl and KCl. After C point, the salt precipitation will continue along the solubility curve. The process is shown in Fig. 20.

4. Conclusions

The phase equilibria of the quaternary system K^+, NH_4^+, Ca^{2+}//Cl^--H_2O at 298.2 K, 323.2 K, and 348.2 K were studied by isothermal dissolution equilibrium method. The equilibrium phase diagrams and multi-temperature comparison diagrams of the system at different temperatures were drawn. The main conclusions are:

(1) The quaternary system K^+, NH_4^+, Ca^{2+}//Cl^--H_2O is a complex system from 298.2 to 348.2 K. There are three invariant points, seven univariate curves and five crystallization phase regions at 298.2 K. The configurations at 323.2 and 348.2 K are the same, with five invariant points, eleven univariate curves, and seven crystallization phase regions.
(2) Compared with 298.2 K, new crystalline regions $2NH_4Cl\cdot CaCl_2\cdot 3H_2O$ and $KCl\cdot CaCl_2$ at 323.2 and 348.2 K. And the crystalline phase region increases with increasing temperature.
(3) The crystal water content of $CaCl_2$ hydrate change with the increase of temperature. It is $CaCl_2\cdot 6H_2O$ at 298.2 K, $CaCl_2\cdot 2H_2O$ at 323.2 and 348.2 K.
(4) In this system, the $(KCl)_x(NH_4Cl)_{1-x}$ solid solution is always the largest crystalline phase region, indicating that the system is easy to form $(KCl)_x(NH_4Cl)_{1-x}$ solid solution, which brings great difficulties to the separation and enrichment of KCl.

CRediT Authorship Contribution Statement

Fuyu Zhuge: Writing – original draft, Data curation. Nan Zhang: Writing – original draft, Data curation. Haiying Tang: Writing – review & editing, Formal analysis. Qi Li: Formal analysis, Writing – review & editing. Niancu Chen: Data curation, Investigation, Validation. Xudong Yu: Writing – review & editing, Supervision, Methodology, Funding acquisition, Conceptualization.

Declaration of Competing Interest

The authors declare that they have no known competing financial interests or personal relationships that could have appeared to influence the work reported in this paper.

Acknowledgements

Supported by the National Key Research and Development Program of China (2023YFC2906503), Sichuan Province Science and Technology Support Program (2023ZYD0036).

References

[1] M.P. Zheng, X.H. Hou, C.Q. Yu, H.P. Li, H.W. Yi, Z. Zhang, X.L. Deng, Y.S. Zhang, The leading role of salt formation theory in the breakthrough and important progress in potash deposit prospecting, *Acta Geosci. Sin.* 36 (2) (2015) 129–139. (in Chinese)

[2] D.B. Hou, M.Y. He, Y.G. Chen, H.Y. Yang, H.M. Li, Application analysis of resource allocation optimization and circular economy in development and utilization of potassium resources, *Chem. Ind. Eng. Prog.* 42 (6) (2023) 3197–3208. (in Chinese)

[3] Assessment report for mineral reserves in the world, Ministry of Natural Resources of the People's Republic of China, 2023.

[4] Z.H. Xiong, S.J. Wang, Overview of potassium resources exploitation & utilization technology and potash industry development, *Conser. Utili. Min. Res.* 40 (6) (2020) 1–7. (in Chinese)

[5] M.P. Zheng, China's Salt Lake Resources and Environment Research, Science Press, Beijing, 2022. (in Chinese)

[6] X. Zhou, Q. Cao, F. Yi, J. Guo, X.C. Wang, S.Y. Zhang, L.D. Wang, Y. Shen, Characteristics of the brines and hot springs in the triassic carbonates in the high and steep fold zone of the Eastern Sichuan Basin, *Acta Geol. Sin.* 89 (11) (2015) 1908–1920. (in Chinese)

[7] X.C. Yu, C.L. Liu, C.L. Wang, H.M. Xu, Y.J. Zhao, H. Huang, R.Q. Li, Genesis of lithium brine deposits in the Jianghan Basin and progress in resource exploration: a review, *Earth Sci. Front.* 29 (1) (2022) 107–123. (in Chinese)

[8] J.H. Han, M.P. Zheng, Z. Nie, T.F. Guo, Q. Wu, Y.S. Wang, Z.D. Cui, T. Ding, Lithium and potassium resources of Oilfield Brine and development prospects in China, *J. Salt Lake Res.* 32 (2) (2024) 90–100. (in Chinese)

[9] W. Li, Y.P. Dong, P.S. Song, Salt Lake Brine Resources Development and Utilization, Chemical Industry Press, Beijing, 2012. (in Chinese)

[10] Y.L. Zhong, J.X. Chen, M. Su, J. Han, Q. Wu, Solid–liquid equilibrium, crystal type, solid solubility and thermal stability studies of potassium ammonium chloride solid solution, *Fluid Phase Equilib* 439 (2017) 24–30.

[11] X.D. Yu, Y. Zeng, Z.X. Zhang, Solid-liquid metastable phase equilibria in the ternary systems $KCl+NH_4Cl+H_2O$ and $NH_4Cl+MgCl_2+H_2O$ at 298.15 K, *J. Chem. Eng. Data* 57 (6) (2012) 1759–1765.

[12] X.D. Yu, L. Wang, J.L. Chen, M.L. Li, Salt–water phase equilibria in ternary systems $K^+(Mg^{2+})$, $NH_4^+//Cl^- - H_2O$ at $T = 273$ K, *J. Chem. Eng. Data* 62 (2017) 1427–1432.

[13] S.Y. Ren, X.D. Yu, J. Luo, X. Feng, Z.X. Zhao, Z.H. Yao, Phase equilibria of aqueous quaternary system Li^+, K^+, $NH_4^+//Cl^-$-H_2O at 298.2 K, *CIESC J.* 73 (10) (2022) 4335–4344. (in Chinese)

[14] D. Ouyang, D.D. Li, D.W. Zeng, A novel eutectic phase-change material: $CaCl_2\cdot 6H_2O + NH_4Cl + KCl$, *Calphad* 63 (2018) 92–99.

[15] S. Wang, B. Zhao, H.F. Guo, T.L. Bai, J.L. Cao, Solid-liquid equilibrium of the NH_4Cl-$MgCl_2$-KCl-H_2O system at 0 °C and its application, *J. Chem. Eng. Chin. Univ.* 31 (3) (2017) 515–520. (in Chinese)

[16] X.L. Zhao, Y.Q. Qin, B. Zhao, Z.Y. Tan, J.L. Cao, Phase equilibrium and application of the KCl-$MgCl_2$-NH_4Cl-H_2O quaternary system at 25 °C, *J. Chem. Eng. Chin. Univ.* 32 (2) (2018) 266–274. (in Chinese)

[17] Q. Li, X.D. Yu, N.C. Chen, X. Feng, Z.X. Zhao, Z.H. Yao, Y.S. Yang, Solid-liquid phase equilibria of potassium-ammonium-magnesium chloride system at 323.2 and 348.2 K, *J. Chem. Eng. Data.* 69 (8) (2024) 2856–2866.

[18] Z.H. Yao, H. Meng, X.D. Yu, S. Chen, J. Luo, Stable phase equilibria of ternary system $KCl+CaCl_2+H_2O$ at 278.2 K and 308.2 K, *Conser. Utili. Min. Res.* 41 (6) (2021) 112–116. (in Chinese)

[19] X.D. Yu, Q. Li, N.C. Chen, L. Du, S.Y. Ren, Y. Zeng, Phase equilibria and calculation of aqueous ternary system $KCl+CaCl_2+H_2O$ at 298.2, 323.2, and 348.2 K, *CIESC J.* 74 (8) (2023) 3256–3265. (in Chinese)

[20] D. Ouyang, D.W. Zeng, H.Y. Zhou, H.J. Han, X. Yin, Y. Du, Phase change materials in the ternary system $NH_4Cl+CaCl_2+H_2O$, *Calphad* 35 (3) (2011) 269–275.

[21] L. Wang, X.D. Yu, M.L. Li, X.L. Cheng, X.J. Tang, Y. Zeng, Phase equilibrium for the aqueous ternary systems NH_4^+, $Sr^{2+}(Ca^{2+})//Cl^-$-H_2O at T=298 K, *J. Chem. Eng. Jpn.* 51 (7) (2018) 551–555.

[22] X.D. Yu, Z.X. Zhao, L. Du, S.Y. Ren, J. Luo, N.C. Chen, Y. Zeng, Phase equilibria of aqueous ternary systems $NH_4Cl+CaCl_2+H_2O$ and $NH_4Cl+MgCl_2+H_2O$ at 308.2 K: measurement and calculation, *J. Chem. Eng. Data.* 67 (12) (2022) 3748–3756.

[23] X.D. Yu, M. Liu, Q.F. Zheng, S. Chen, F. Zou, Y. Zeng, Measurement and correlation of phase equilibria of ammonium, calcium, aluminum, and chloride in aqueous solution at 298.15 K, *J. Chem. Eng. Data* 64 (8) (2019) 3514–3520.

[24] S. Feng, X.D. Yu, J. Luo, Q.F. Zheng, M. Liu, Stable phase equilibrium experiment of quaternary system NH_4Cl-$CaCl_2$-$SrCl_2$-H_2O at 298.2 K, *J. Chem. Eng. Chin. Univ.* 37 (2) (2023) 194–201. (in Chinese)

[25] J. Luo, S.Y. Ren, Q.F. Zheng, X.D. Yu, Solid-liquid phase equilibria determination of quaternary system NH_4^+, Mg^{2+}, $Ca^{2+}//Cl^-$-H_2O at T=298.2 and 323.2 K and p=94.77 kPa, *J. Chem. Eng. Data* 68 (3) (2023) 769–779.

[26] Methods for Chemical Analysis of Aluminium and Aluminium Alloys-Part 33: Determination of Potassium Content-Flame Atomic Absorption Spectrometric Method, Standards Press of China, Beijing, 2020 [GB/T 20975.33—2020].

[27] Industrial Circulating Cooling Water-Determination of Sodium, Potassium, Ammonium and Calcium-Ion Chromatography [GB/T 15454—2009], Standards Press of China, Beijing, 2009.

[28] Methods for Chemical Analysis of Aluminium and Aluminium Alloys-Part 21: Determination of Calcium Content-Flame Atomic Absorption Spectrometric Method, Standards Press of China, Beijing, 2020 [GB/T 20975.21—2020].

[29] Institute of Qinghai Salt Lakes of Chinese Academy of Science, Analytical Methods of Brines and Salts, Science Press, Beijing, 1988. (in Chinese)

[30] L.Z. Zhang, Q.L. Gui, X.H. Lu, Y.R. Wang, J. Shi, B.C.Y. Lu, Measurement of solid–liquid equilibria by a flow-cloud-point method, *J. Chem. Eng. Data* 43 (1) (1998) 32–37.

[31] J.S. Yuan, X. Li, Y.L. Liu, Study on phase equilibrium of NH_4Cl-$CaCl_2$-H_2O ternary system, *Ind. Miner. Process.* 39 (6) (2010) 4–8. (in Chinese)